eLife

Reviewed Preprint
v1 • December 13, 2024
Not revised

Reviewed Preprint
v2 • February 27, 2026
Revised by authors

For correspondence: blumem@rki.de

Competing interests: No competing interests declared

Funding: See page 29

Reviewing editor: Bavesh D Kana, University of the Witwatersrand, South Africa

Screening the MMV Pathogen Box reveals the mitochondrial bc_1-complex as a drug target in mature *Toxoplasma gondii* bradyzoites

Deborah Maus[1], Elyzana Putrianti[1], Tobias Hoffmann[3], Michael Laue[3], Frank Seeber[2], Martin Blume[1]

[1]P 6: Metabolism of Microbial Pathogens, Robert Koch Institute, Berlin, Germany • [2]FG 16: Mycotic and Parasitic Agents and Mycobacteria, Robert Koch Institute, Berlin, Germany • [3]ZBS 4: Advanced Light and Electron Microscopy, Centre for Biological Threats and Special Pathogens 4, Robert Koch-Institute, Berlin, Germany

eLife Assessment

This **valuable** study utilizes a newly developed approach to culture T gondii bradyzoites in myotubes, and then takes advantage of the antiparasitic compound collection known as the Pathogen Box, to find compounds that target both tachyzoite and bradyzoite forms of the parasite. A set of compounds yielding patterns consistent with targeting the mitochondrial bc1 complex was explored further, with **solid** evidence for changes in ATP production in bradyzoites to support the conclusions about the importance of this complex. The paper will be interesting for parasitologists studying drug discovery of apicomplexan parasites.

https://doi.org/10.7554/eLife.102511.2.sa4

Abstract

The apicomplexan parasite *Toxoplasma gondii* infects 25-30% of the global human population and can cause life-threatening diseases in immunocompromised patients. The chronically infectious forms of the parasite, bradyzoites, persist within cysts in brain and muscle tissue and are responsible for its transmission and remission of the disease. Currently available treatment options are very limited and are only effective against the fast-replicating tachyzoites but fail to eradicate the chronic stages of *T. gondii*. The cause of these treatment failures remains unclear. Here, we utilized our recently developed human myotube-based culture model to screen compounds from the MMV Pathogen Box against pan-resistant in vitro bradyzoites and identified multiple compounds with simultaneous activity against tachyzoites and bradyzoites. Stable isotope-resolved metabolic profiling on tachyzoites and bradyzoites identified the mitochondrial bc_1-complex as a target of bradyzocidal compounds and defines their metabolic impacts on both parasite forms. Our data suggest that mature bradyzoites rely on mitochondrial ATP production.

Introduction

Toxoplasma gondii is an ubiquitous apicomplexan parasite that infects virtually all warm-blooded animals, including 25-30 % of humans (Montazeri et al. 2020). Of all food-borne pathogens, *T. gondii* causes 20% of the total disease burden in Europe (Havelaar et al. 2015). Although most acute infections caused by the fast replicating tachyzoite stage of the parasite remain asymptomatic in immunocompetent individuals, the parasite persists life-long in the form of encysted semi-dormant bradyzoites (Weiss and Dubey 2009). Currently, no medical treatment exists to eradicate these tissue cysts with their rigid cyst wall from infected individuals. *T. gondii* is transmitted through undercooked meat products of infected livestock but also via feline-shed oocysts that can contaminate water sources and soil (Weiss and Dubey 2009). Severe

toxoplasmosis occurs after reactivation of cysts or primary infection of immunosuppressed individuals or fetuses of seronegative mothers and can lead to systemic infections, uveitis, encephalitis as well as congenital transmission with potentially fatal outcomes (Montoya and Liesenfeld 2004). Hence, tissue cysts of *T. gondii* constitute a long-term source for transmission and risk of acute disease. Also, other related cyst-forming coccidian parasites such as *Neospora caninum* and *Besnoitia besnoiti* pose an immense veterinary burden by causing abortion mainly in sheep and severe chronic infections in cattle and horses, respectively. Current treatment options exist only against the tachyzoite form of these parasites and include antifolates, such as pyrimethamine or trimethoprim, that inhibit the bifunctional dihydrofolate reductase-thymidylate synthetase, in combination with sulfadiazine, which blocks the dihydropteroate synthetase. These enzymes are implicated in DNA synthesis in both the parasite and side-effects often require premature termination of the treatment (Katlama, De Wit, et al. 1996; Alday and Doggett 2017). Another potent drug target in coccidians and other apicomplexan parasites such as *Plasmodium* spp. is the cytochrome bc_1-complex in the mitochondrial respiratory chain, which is inhibited by a number of approved drugs, such as the naphthoquinones atovaquone (ATQ) (Meneceur et al. 2008; Nixon et al. 2013) and buparvaquone (BPQ) (Sharifiyazdi et al. 2012). However, both coenzyme Q analogs including bioavailable nanosuspensions (Shubar et al. 2011) fail to eradicate encysted bradyzoites of *T. gondii* and *N. caninum* from the brains of infected mice after multiple weeks of treatment (Doggett et al. 2012; Müller et al. 2015; Doggett et al. 2020). Experimental inhibitors of the bc_1-complex includes 1-hydroxy-2-dodecyl-4(1H)quinolone (HDQ) that arrests the growth of asexual blood stages of the related malaria parasite *P. falciparum* (Vallières et al. 2012). However, in *T. gondii* HDQ appears to inhibit multiple mitochondrial election donors such as the alternative NAD-dehydrogenase and the dihydroorotate dehydrogenase in tachyzoites (S. S. Lin, Gross, and Bohne 2009). It does not affect mature bradyzoites in vitro (Christiansen et al. 2022), and HDQ derivatives do not clear *T. gondii* cysts from the brain of infected mice (Bajohr et al. 2010). In addition, endochin-like quinolones constitute a promising series of potent bc_1-complex inhibitors that are active against *T. gondii* (McConnell et al. 2018) and *Plasmodium* parasites (Song et al. 2018). However, these compounds also do not fully eradicate the cysts *in vivo* (Doggett et al. 2012, 2020). Similarly, bumped kinase inhibitors that selectively inhibit parasite calcium-dependent protein kinases in various apicomplexans fail to clear tissue cysts *in vitro* (Christiansen et al. 2022) and *in vivo* (Hulverson et al. 2019). Despite these efforts, it remains unclear whether the target proteins of these drugs are rendered dispensable for the survival of bradyzoites or whether the eradication failures have other reasons, such as poor permeability across the blood brain barrier and/or the cyst wall. To date, the genetic tools available to directly characterize the function of essential genes in bradyzoites are limited to promoter replacements (Smith et al. 2021), while no genetic methods exist to directly interrogate the fitness contribution of mitochondrially encoded genes such as the cytochrome b subunit of the cytochrome bc_1-complex (J.-L. Wang et al. 2016). Consequently, reverse pharmacological approaches, that involve screening of inhibitors against target proteins, remain difficult and the underlying reasons for limited *in vivo* efficacies remain uncertain.

Here we aim to address these shortcomings and identify essential processes in bradyzoite by a combination of a phenotypic screen and subsequent metabolomics-driven identification of the modes of actions of hit compounds. We employed a recently developed human myotube-based culture system to generate mature *T. gondii* drug-tolerant bradyzoites (Christiansen et al. 2022; Maus et al. 2024) to screen the MMV Pathogen Box. These *in vitro* cysts exhibit resistance against antifolates, bumped kinase inhibitors and HDQ. They also express hallmarks of *in vivo* cysts including oral infectivity and a cyst wall (Christiansen et al. 2022). The Medicines for Malaria Venture (MMV) Pathogen Box provides a curated set of bioactive molecules with activity against a number of pathogens including *P. falciparum*, *Cryptosporidium parvum*, *Shistiosoma spp.* and diseases caused by kinetoplastids (Veale 2019). Untargeted and stable isotope-resolved metabolomic analyses of active drugs identified established and unsuspected modes of action in tachyzoites and bradyzoites, respectively. Our data directly show metabolic consequences of bc_1-complex inhibition in bradyzoites and suggest its crucial role in ATP production.

Material and methods

Tachyzoite Culture

Pru-Δhxgprt tdTomato (John et al. 2009) (PruTom) and RH-Rep1/2-S9(33-159)-GFP (DeRocher et al. 2000; Thomsen-Zieger, Schachtner, and Seeber 2003) (RH-S9) parasites were maintained in human foreskin fibroblasts (HFF) cells (BJ-5ta human foreskin fibroblasts ATCC, CRL-4001) with Dulbecco's modified Eagle's medium (DMEM) containing 25 mM glucose, 4 mM L-glutamine, 1 mM sodium pyruvate, 100 U/mL penicillin, 100 µg/mL streptomycin and 1 % heat-inactivated fetal bovine serum (FBS, Gibco) at 37°C with 10 % CO_2 (Christiansen et al. 2022).

In vitro T. gondii tissue cyst culture

The *T. gondii in vitro* cyst culture was performed as in (Christiansen et al. 2022; Maus et al. 2024). In short, KD3 myoblasts (Shiomi et al. 2011) were grown to 70 % confluency, followed by the induction of myotube differentiation by changing the medium to DMEM as described above but with 2% horse serum instead of FBS and additionally supplemented with 10 µg/mL human insulin, 5 µg/mL human holo-transferrin and 1.7 ng/mL Na_2SeO_3. After five days, the myotubes were infected with PruTom (MOI 0.1) in bicarbonate-free Roswell Park Memorial Institute medium (RPMI) containing 5.5 mM glucose, 50 mM HEPES, 4 mM L-glutamine, 100 U/mL penicillin, 100 µg/mL streptomycin, 2 % horse serum, 10 µg/mL human Insulin, 5 µg/mL human holo-transferrin and 1.7 ng/mL Na_2SeO_3. Cultures were incubated at 37 °C at ambient CO_2 for four weeks and the medium was changed every two to three days. A comprehensive scheme of the procedure is shown in Fig. S1.

MMV Pathogen Box Screening Procedure

All Pathogen Box compounds were stored at −20°C (Veale 2019). DMSO-solved compounds were diluted in DMEM or RPMI media and stored at 4°C until use. Host cells were grown in transparent, flat-bottom 96-well plates and infected as described above to cultivate either tachyzoites or in vitro tissue cysts. One column per plate was left uninfected to estimate fluorescence background. Four hours after infection with tachyzoites or after four weeks of bradyzoite maturation the culture medium was replaced by medium containing either 0.1 % DMSO (negative control) or 10 µM of the respective Pathogen Box compound. During the seven-day treatment period the medium was renewed every two to three days. It was then changed to tachyzoite growth medium to induce re-differentiation of viable bradyzoites to tachyzoites, and then the culture was monitored over 28 days. Prior to each medium exchange, the cultures were monitored for compound crystallization. The fluorescence was measured in a fluorescence plate reader (Tecan Infinite M200 PRO) (excitation Λ = 554 nm, emission Λ = 589 nm). Fluorescence values passing a threshold of 2,000 after background subtraction indicated proliferating parasites and hence an ineffective treatment (Fig. 1).

Resazurin viability assay and cytotoxicity

After the growth assays were completed, the host cell monolayers of both HFF and KD3 myotubes were washed with PBS and incubated with 500 nM resazurin in Milli-Q water at 37 °C for 4 hours. Fluorescence was measured (excitation Λ = 540 nm, emission Λ = 580 nm) in a fluorescence plate reader and normalized to the average fluorescence values of the DMSO-treated controls, which were set at 100 %. During bradyzoite assays KD3 host cells were visually inspected after drug exposure for one week. After completion of the re-growth phase for four weeks the colorimetric resazurin was performed. These values were reported as lowest cytotoxicity values (Supplemental Fig 2D). During secondary tests of putatively dually active compounds resazurin assays were performed in a concentration dependent manner (Supplemental File S1, Supplemental Fig 2D).

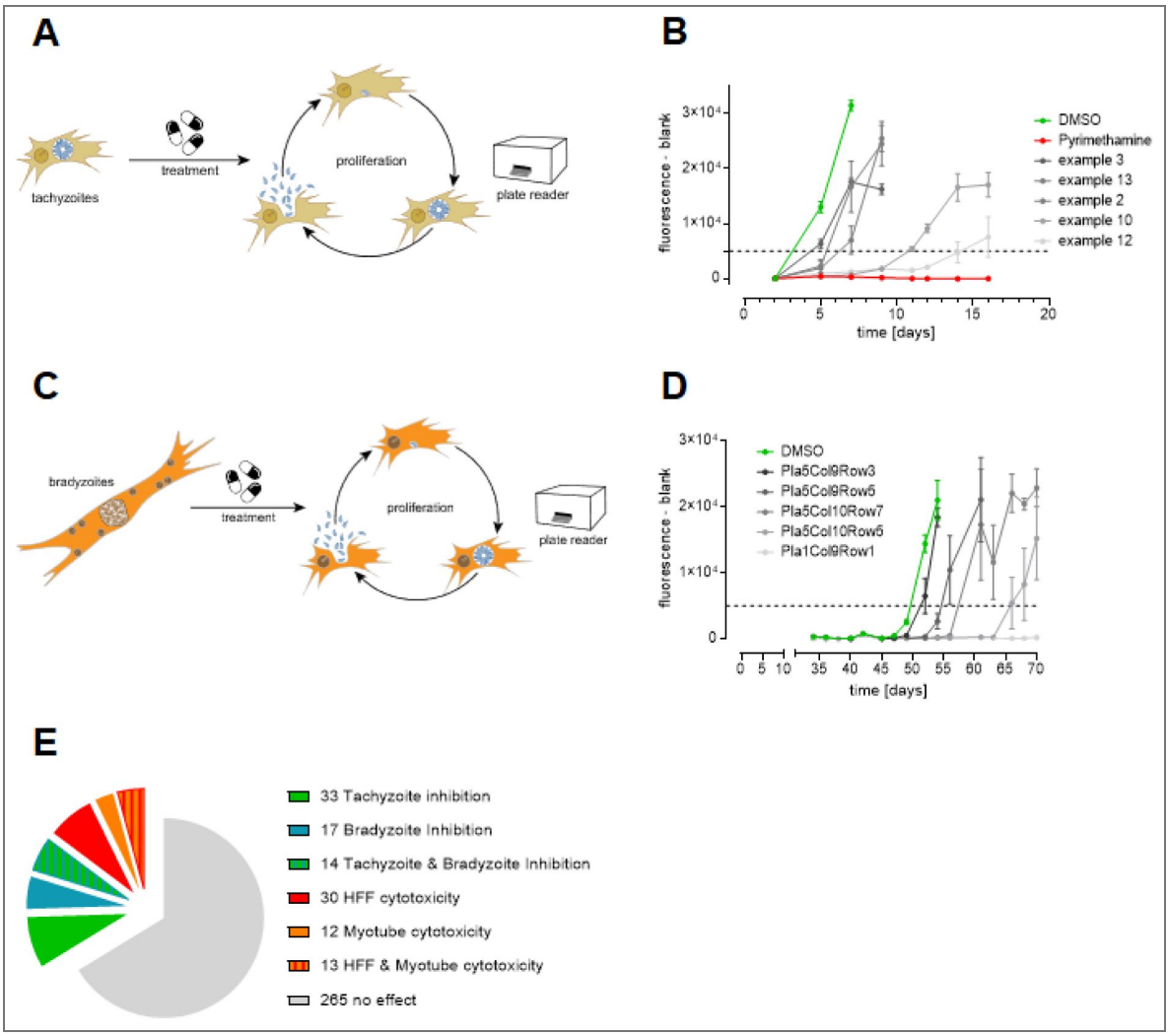

Figure 1. An in vitro screen reveals tachy- and bradyzocidal properties of the MMV Pathogen Box compounds.

(A) Experimental scheme of the MMV compound screen on *Toxoplasma gondii* tachyzoites in human foreskin fibroblast cells (B) Growth curves of tachyzoites treated with 10μM of each MMV compound for 7 days (shades of grey), a solvent control (green), and an inhibition control (red) (C) Experimental scheme of the MMV compound screen on bradyzoites matured in myotubes (D) Growth curves of bradyzoites treated with 10μM of each compound (shades of grey) or a solvent control (green) for 7 days, followed by a tachyzoite regrowth phase (E) Pie chart displaying the number of Pathogen Box compounds and their effects on our in vitro cultures.

The dose response of dually active compounds

For the measurement of LC50 and minimal lethal concentrations tachyzoite and bradyzoite cultures were treated with the MMV compounds which were pipetted in a serial dilution across the 96-well plate and treated for 7 days. Afterwards, the compound containing medium was removed and possible regrowth was monitored for another 7 days (tachyzoite assay) or 21 to 28 days (bradyzoite assay) in a fluorescence plate reader (Tecan Infinite M200 PRO) (excitation Λ = 554 nm, emission Λ = 589 nm). The relative fluorescence units were background-subtracted. Depending on the development of the DMSO control, a late timepoint when DMSO-treated cultures still continued exponential growth was chosen to calculate the half-maximal inhibitory concentration (IC_{50}) for tachyzoites. This time point was between day 4 and 7. Bradyzoite cultures were of lower MOI, and we calculated LC_{50} values between experiments from 7 to 28 days post treatment when exponential growth occurred in mock treated cultures (Fig. 2). The concentration data was log-transformed and a non-linear regression (curve fit with variable slope) was performed to determine the dose response (Prism 9, GraphPad).

In silico predictions

MMV provided the SMILES IDs for every compound, which were compiled with LightBBB (Shaker et al. 2020) to predict the blood-brain permeability. SwissADME (Daina, Michielin, and Zoete 2017) was used to predict the gastrointestinal absorption capability. The logP values (Fig. S2) were provided by MMV and remaining logP values were calculated on SwissADME (Daina, Michielin, and Zoete 2017) as consensus values.

Fluorescence stain of mitochondrial activity

This assay was performed on tachyzoites and bradyzoites. For the tachyzoite experiment, HFF cells were infected with RH-S9 parasites at an MOI 0.1 and treated for 24 h with 1 µM atovaquone, 25 nM buparvaquone or 5 µM MMV1028806, respectively, corresponding to five-fold of the respective IC_{50} values, or 0.1% DMSO as a solvent control. For the bradyzoites experiment, 4 weeks-old ME49 *in vitro* cysts were treated for 24h with 5 µM atovaquone, 500 nM buparvaquone or 5 µM MMV1028806, respectively, corresponding to the lowest lethal concentration, or 0.1 % DMSO as a solvent control.

The assay was repeated with additional control treatments (see Supplemental Fig S5). In this experiment, HFF cells were infected with RH-S9 tachyzoites and, 4h post-infection, incubated for 24h with 0.1% DMSO (solvent control), 1 µM atovaquone, 25 nM buparvaquone, 5µM MMV1028806 (MMV), 1 µM pyrimethamine (Pyri), 10 nM clindamycin, or 25 µM 6-diazo-5-oxonorleucine (DON). Concentrations reflected the five-fold IC_{50} values, except for DON, which does not inhibit growth.

Subsequent staining and imaging procedures were identical across all experiments. Cultures were then stained with 500 nM MitoTracker Deep Red FM (MT; Thermo Fisher) in DMEM for 40 min at 37 °C, followed by a 20 min de-staining with DMEM and final fixation with 1 % paraformaldehyde for 20 min at room temperature. The cyst wall was decorated with Dolichos Biflorus Agglutinin (DBA) and stained with Streptavidin-Cy2. Mowiol containing DAPI (1:3,000) was used to mount the cells. To avoid a biased image acquisition, all parasite vacuoles or cysts identified in a specimen along an horizontal axis were imaged. Tachyzoite images were taken with a Zeiss Axio Imager Z1 Microscope equipped with the ApoTome 2 at identical exposure times (DAPI 200 ms, MT 500 ms, S9-GFP 200 ms, Brightfield 10 ms) using a Zeiss Plan APOCHROMAT 63x/1.4 oil objective lens. Bradyzoite images were acquired on a Leica Stellaris 8 laser scanning confocal microscope using a Leica HC PL APO CS2 63x/1.4 oil objective lens. The pinhole diameter was set to 1 AU. All detectors were operating in photon counting mode. The acquisition parameters were set as follows. DAPI: diode laser at $405nm_{exc}$ with 2.2%, $430\text{-}550nm_{em}$ with a HyD S-detector. Cy2: WLL at $468nm_{exc}$ with 8.5%, $473\text{-}591nm_{em}$ with a HyD S-detector. MitoTracker: WLL at $641nm_{exc}$ with 2.7%, $650\text{-}784nm_{em}$ with a HyD X-detector (4x line average). The zoom was set to 7x, images were acquired in frame-sequential mode with a unidirectional scan speed of 400 Hz, the pixel dwell time for all channels was 3.18µs. For z-Stacks, z-step size was set to 0.299 µm.

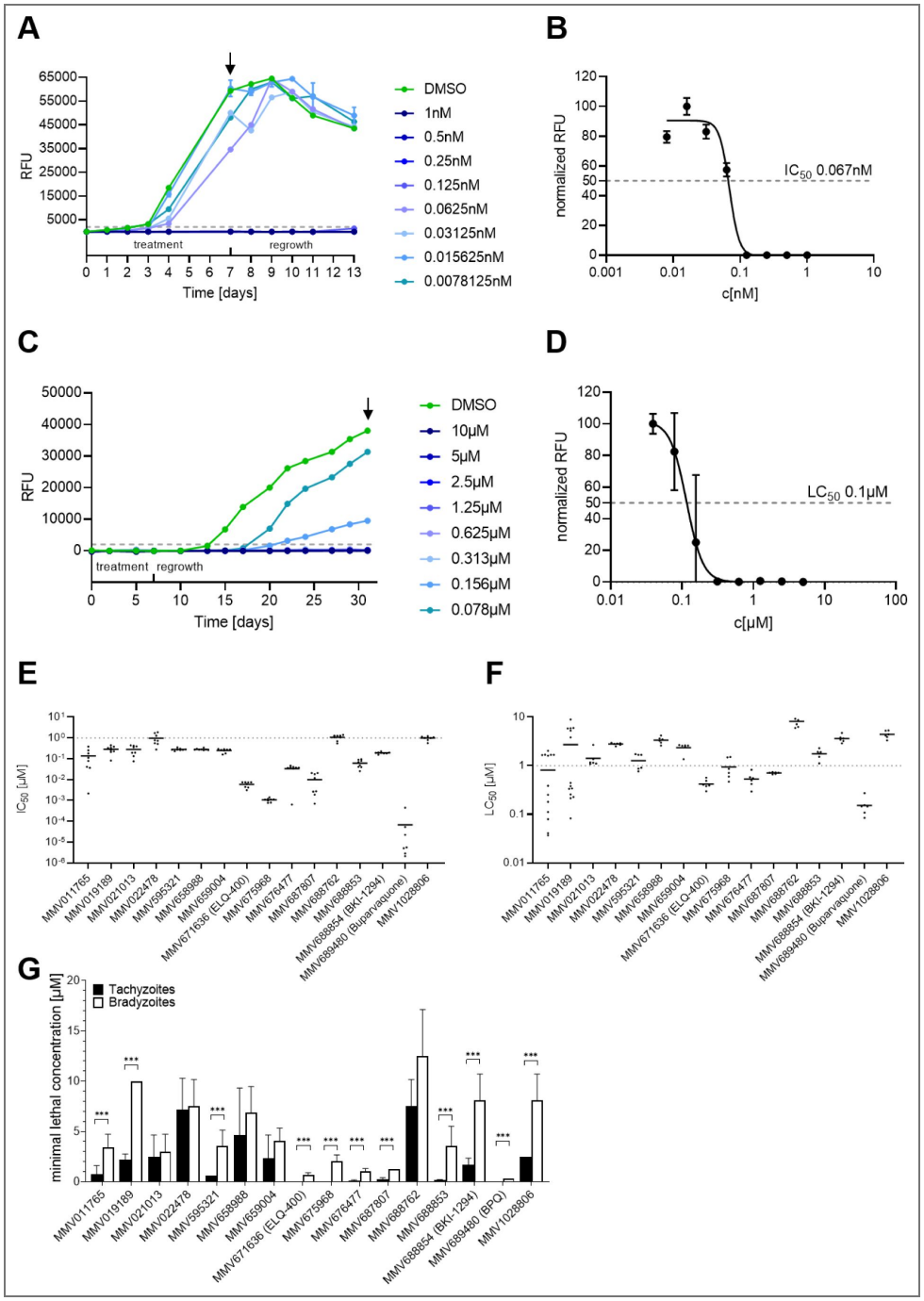

Figure 2. Confirmed Pathogen Box compounds that target both tachyzoites and mature bradyzoites.

(A) shows the growth curve of MMV689480 (Buparvaquone), one of the 16 dually active compounds, in a tachyzoite growth assay (n=8). The infected cultures were treated for 7 days and regrowth in absence of the inhibitor was observed for another week. Depending on the development of the DMSO control, the half-maximal inhibitory concentration (IC_{50}) was determined at either day 4 or 7 (arrow). (B) shown is the respective data plotted as relative fluorescence units depending on the concentration at day 7. (C) With 4 weeks old, mature bradyzoite cultures (n=6), the half-maximal lethal concentration (LC_{50}) was determined at the time point which ideally reflected the dose-response curve (in the case of Buparvaquone at day 31; arrow). (D) The LC_{50} of Buparvaquone on encysted bradyzoites determined at day 31. All IC_{50} and LC_{50} of dually active compounds are summarized in (E) for tachyzoite and (F) for bradyzoite cultures. The grey dotted line indicates 1 µM in both charts. (G) Comparison of the minimal lethal concentration of each compound on tachyzoites and bradyzoites. Mann-Whitney test of eight replicative measurements on tachyzoites and six replicates of bradyzoites from two independent experiments each *** $p < 0.001$.

Using ImageJ (Schindelin et al. 2012), the intensity threshold of individual pixels of MT (190 to 255 for tachyzoites and 125 to 65535 for bradyzoites) and DAPI (140 to 255 for tachyzoites and 363 to 65535) channels was cut off and the signal intensity was calculated per parasitophorous vacuole or cyst.

Oxygen consumption assay

To assess mitochondrial oxygen consumption in *T. gondii* RHku80 tachyzoites, we employed the MitoXpress Xtra Oxygen Consumption Assay (Agilent Technologies, Cat# MX-200-4) following the manufacturer's high-sensitivity (HS) method with modifications. Parasites were freshly harvested upon egress and resuspended at a density of 1×10^7 tachyzoites per reaction in phenol red-free D1 medium lacking glucose but supplemented with glutamine to promote mitochondrial electron transport chain (mETC) activity via the GABA shunt (MacRae, Sheiner et al. 2012).

Parasites were incubated in medium with one of the following treatments: 0.1% DMSO (vehicle control), 1 µM antimycin A (complex III inhibitor, positive control), 10 µM FCCP (uncoupler, commonly used to determine the maximum respiration capacity), 1 µM ATQ, 1 µM BPQ, or 1 µM MMV1028806. Untreated control wells contained 1×10^7 tachyzoites in 0.1% DMSO. Background fluorescence was determined from wells containing MitoXpress Xtra reagent but no parasites.

Each 100 µL reaction was supplemented with 10 µL of reconstituted MitoXpress Xtra reagent. To prevent oxygen diffusion from ambient air, 100 µL of prewarmed HS mineral oil was carefully layered over each well. Plates were immediately transferred to a prewarmed Tecan Infinite 200 Pro plate reader, maintained at 37 °C. Fluorescence was recorded every 2 minutes for 2 hours using the following settings: excitation at 380 nm, emission at 650 nm, gain 220, 25 flashes, 30 µs integration delay, and 100 µs integration time.

Data were analyzed by determining the slope of the fluorescence lifetime signal (indicative of oxygen consumption) after an equilibration period of 20 minutes. The linear portion of the curve (typically over a 60-minute window) was used for slope determination. Background signal from cell-free wells was subtracted from all conditions to obtain net oxygen consumption rates. Data was normalized to the untreated control.

Thin section electron microscopy

The *T. gondii in vitro* cyst culture was performed as described above. After four weeks, cells were treated with 5 µM atovaquone, 500 nM buparvaquone, 5 µM MMV1028806, corresponding to the lowest lethal concentration, or 0.1% DMSO, as a solvent control, for 24h. Cells were fixed by covering the monolayer with a fixation solution of 1% paraformaldehyde and 2.5% glutaraldehyde (Electron Microscopy Services) in 0.05 M HEPES buffer (pH 7.4). After incubation at RT for 3h, samples were sealed with parafilm and stored in the fridge until further processing. Fixed cells were scraped, sedimented by centrifugation (3000 *g*, 10 min) using a swing-out rotor and washed twice with 0.05 M Hepes buffer. The cell sediment was embedded in low melting-point agarose and stored in 2.5% glutaraldehyde in 0.05 M HEPES buffer. Small blocks of the embedded sediment were subjected to postfixation (osmium tetroxide, tannic acid), *en bloc* contrasting (uranyl acetate), dehydration, and embedding in epoxy resin according to a standard protocol (Laue 2010).

Ultrathin sections were prepared with an ultramicrotome (UC7, Leica Microsystems, Germany) using a diamond knife (45°, Diatome, Switzerland). The sections were collected on bare copper grids (300 mesh, hexagonal mesh shape) or copper slot grids, contrasted with 2% uranyl acetate and 0.1% lead citrate, and coated with a thin (2-3 nm) layer of carbon. The ultrathin sections with a thickness of ~65 nm were examined with a transmission electron microscope (Tecnai Spirit, Thermo Fisher Scientific) operated at 120 kV. Images were recorded with a side-mounted CCD camera (Phurona, EMSIS, Germany) at 4095 x 2984 pixels.

Metabolomic analysis of drug-treated intracellular tachyzoites and bradyzoites

HFF cells were infected with PruTom at MOI 1. Approximately 64 h later, the cultures were treated with 1.5 µM MMV019189, 7 µM MMV1028806, 30 µM MMV228911, 1.2 µM MMV595321, 5 µM MMV688762, 2 µM MMV688854, respectively, and 0.1 % DMSO as a control for 3h. These concentrations correspond to the five-fold respective IC_{50} value. Cultures were quenched in ice-cold PBS and parasites were isolated from their host cells by passaging scraped monolayers through a 23G needle, filtered through a 3 µm polycarbonate filter and after microscopic counting distributed at 1 x 10^8 parasites per sample. Parasites were washed with ice-cold PBS via 5 min centrifugation at 21,500 x *g* at 0 °C. Metabolites were then extracted by sonication for 2 min in 50 µL 80 % acetonitrile in water. The insoluble particles were pelleted for 5 min at 21,500 x *g* at 0 °C. 5 µL of each sample was collected to generate a pooled biological quality control (PBQC) which was injected regularly within the otherwise randomized run list. 5 µL of each sample was injected onto either an ACQUITY UPLC BEH amide column (Waters) equipped with a VanGuard amide pre-column (Waters) or onto a SeQuant ZIC-pHILIC (Merck) column with an OPTI-LYNX ZIC-pHILIC guard column cartridge (Optimize Technologies) operating on a Vanquish Flex (Thermo Fisher). Analytes were chromatographically separated starting with 100 % eluent A (90 % acetonitrile in water with 10 mM ammonium carbonate) and 0 % eluent B (10 mM ammonium carbonate in water), decreasing to 40% A and 60% B over 25 min. Metabolites were detected on a Q Exactive Plus (Thermo Fisher) equipped with an electrospray ionization source operated in rapid polarity-switching mode at an MS^1 resolution of 70k and an MS^2 resolution of 35k (Top3 MSX1). Peak extraction, retention time alignment, and peak annotation were computed with Compound Discoverer 3.1 (Thermo Fisher) using an in-house library of authentic standards. Blank subtraction, gap-filling as well as statistical analysis were performed in Excel (Microsoft), and the data was plotted with GraphPad Prism 8.4.1. Principal component analysis was performed with ClustVis (Metsalu and Vilo 2015).

Isotopic labeling

Intracellular parasites were treated as mentioned above and incubated for three hours with DMEM containing either 25 mM U-^{13}C-glucose or 4 mM ^{15}N-amide-glutamine instead of the respective unlabeled carbon sources. Quenching, parasite isolation, metabolite extraction and liquid chromatography were performed as described. To increase coverage of the isotopologues, metabolites were measured in positive and negative mode separately without MS^2 scans but with an increased MS^1 scan resolution of 140k. For peak identification purposes, the unlabeled DMSO-treated sample was analyzed with intermittent MS^2 scans as described above.

ATP luciferase assay

PruTOM tachyzoites were cultivated in HFF cells without glucose, isolated 48 h post-infection and treated with 1 µM atovaquone or HDQ for 3h. PruTOM bradyzoites were matured for three weeks, glucose-starved for an additional week and treated for 24 h with 1 µM atovaquone or HDQ before being released by needle passage 23G, pepsin digestion for 20 min at 37 °C. The digestion reaction was stopped by neutralizing in 1.2 % sodium bicarbonate (pH ≈ 8.3) with 0.0159 g/l phenol red as pH indicator dye (Christiansen et al. 2022). They were isolated by douncing on ice and filtered through a 3 µm polycarbonate filter. 10^5 parasites were then aliquoted in 100 µL ice-cold PBS in a 96-well plate. ATP was quantified using BacTiter-Glo™ Microbial Cell Viability Assay (Promega) according to the manufacturer's protocol using a standard curve. Data were plotted in GraphPad Prism 8.4.1..

Metabolomic analysis drug responses on *in vitro* cysts

Intracellular cysts were isolated from their myotube host cells and extracted as described in (Christiansen et al. 2022; Maus et al. 2024). In short, cysts were released by needle passage (23G) and captured with DBA-coated magnetic beads. PBS (with 2% BSA) washed cysts were

extracted in 80% acetonitrile and analyzed as described above. One dish yielded approximately 10^6 cysts and was distributed into 3 samples. Prior to a statistical analysis, the dataset was normalized by dividing the compound intensities through the summed intensities of the respective samples.

Results

The Pathogen Box contains dually active compounds

To initially identify compounds that simultaneously target the tachyzoite and the bradyzoite stage of *T. gondii*, we tested 371 of 400 compounds from the Pathogen Box at a concentration of 10 µM against both stages. We excluded previously reported active compounds against *T. gondii* tachyzoites (Spalenka et al. 2018) from this initial screen. HFF cells were infected with tachyzoites of the Pru strain expressing tandem Tomato fluorescent protein in its cytosol (PruTom) at an MOI of 1 (Fig. 1A). 47 compounds completely inhibited growth during 7 days of exposure while the parasitemia of DMSO-treated controls already peaked after 4 days (Fig. 1B). To also identify bradyzocidal compounds, we differentiated KD3 myoblasts for one week into multinucleated myotubes and infected them under bicarbonate-deplete conditions and at a multiplicity of infection of 0.1 for four weeks to allow maturation of tissue cysts (Fig. S1). We exposed the cultures to 10 µM of the 371 MMV compounds for one week, removed the inhibitors and stimulated re-differentiation into tachyzoites by bicarbonate supplementation (Fig. 1C). Growth of DMSO-treated cultures became detectable after 10 to 14 days. Interestingly, 31 compounds prevented any tachyzoite regrowth (Fig. 1D), indicating their bradyzocidal activity. To exclude host cytotoxicity-dependent suppression of parasite growth, we measured cell viability via the reductive potential of myotubes and HFF cells using a resazurin assay. At 10 µM, 30, 12 and 13 compounds inflicted cytotoxicity onto HFFs, myotubes or both cell types, respectively (Supplemental File 1). This initial screen identified 14 compounds with activity against both tachyzoites and bradyzoites and no apparent cytotoxicity (Fig. 1E).

Validation of screening hits

To validate our results, we determined half-inhibitory concentrations (IC_{50}) in PruTom tachyzoites (Fig. 2A, B) and half-maximal lethal concentration (LC_{50}) in bradyzoites. We also included 29 compounds that were previously reported to target tachyzoites (Spalenka et al. 2018). We confirmed dual activity of 16 compounds that exhibited mean IC_{50} values ranging between 70 pM and 1.1 µM for tachyzoites (Fig. 2E, Fig. S2D) and LC_{50} values between 0.15 and 8.2 µM for bradyzoites (Fig. 2F, Fig. S2D). To allow a comparison between the tachyzoite and bradyzoite data, we also determined the respective minimal lethal concentrations (MLC) over a seven-day treatment duration of tachyzoites as well (Fig. 2G). Except for four not significantly different compounds (MMV021013, MMV022478, MMV658988, MMV65900), minimal lethal concentrations appear generally higher in bradyzoites, potentially reflecting their lower metabolic activity and/or the cyst wall as a diffusion barrier.

Dually active MMV Pathogen Box hits share high lipophilicity and are indicated to be active against other pathogens

To gain insight into general properties of active compounds from our initial screen (Fig. 1E), we tabulated indicated activities as provided by MMV (Fig. S2A, D). As expected, these compounds were mostly earmarked as active against *T. gondii* tachyzoites (67%), however, none of those compounds exhibited bradyzocidal activity. Instead, 27% of dually active compounds were considered active against *Cryptosporidium*. Also, despite the relative phylogenetic proximity of *P. falciparum*, only 5% of the 125 potential antimalarials blocked growth of both *T. gondii* stages. To characterize physicochemical properties of these dually active hits, we approximated their lipophilicity by their logP values (Supplemental File 1) and compared them to compounds that were inactive against *T. gondii* (Fig. S2B). We found that tachyzocidal, bradyzocidal and dually active compounds possess a statistically significantly higher lipophilicity and this trend appeared

more accentuated for bradyzocidal and dually active compounds. However, when comparing tachyzocidal with bradyzocidal compounds, including dually active ones, we did not find a difference (p = 0.06). We estimated permeability through the blood brain barrier (bbb) using LightBBB (Shaker et al. 2020) and gastrointestinal absorbability using swissADME (Daina, Michielin, and Zoete 2017) (Supplemental File 1). Most of the dually active drugs were predicted to be both permeable across the bbb and absorbed in the intestine (Fig. S2C). Together, these data support phylogenetic relationship as a weak predictor of activity of Pathogen Box compounds against *T. gondii* bradyzoites and highlight the role of lipophilicity among the compounds tested here.

Metabolic drug responses in tachyzoites indicate conserved and novel modes of action

We chose to focus on dually active compounds, because they are clinically more relevant and investigation of their targets allows comparisons between on parasite stages. To that end, we choose five compounds based on their availability and yet unknown mode of action (Fig. 3, Supplemental File 2, Fig S3C) to test metabolite responses of tachyzoites. Infected monolayers were treated for three hours with compound concentrations five times their respective IC_{50} values or the solvent DMSO. The inhibitor MMV688854 (BKI 1294) (Doggett et al. 2014) is considered to inhibit a non-metabolic target (calcium-dependent protein kinase (CDPK1)) at the employed concentration (Hayward et al. 2023) and served as an additional control to estimate the metabolic impact of growth inhibition. We filter-purified parasites from quenched monolayers and analyzed their acetonitrile extracts by LCMS using both, pHILIC and BEH-amide chromatography columns. We generated 9 samples per condition from three repeats of the experiment with triplicate samples. A principal component analysis illustrates that batch effects are the main contributors to biological variances within the dataset (Fig. S3A, B). Despite that, all compounds elicited a distinct metabolic phenotype on both LCMS systems (Fig. 3). The CDPK1 inhibitor increased levels of AMP, oxidized glutathione, pseudouridine, citrulline, glycolate and glutamyl glutamine, while reducing the abundances of GABA, carbamoyl aspartate, phosphoenolpyruvate and a hexose phosphate. Shifts in these metabolites are shared among many treatments and indicate their implication in a general stress response and thus do not signify direct interference with parasite metabolism.

Inhibitor-specific responses include the accumulation of cGMP-AMP after treatment with MMV019189, accumulation of carbamoyl aspartate and dihydroorotate upon MMV1028806 treatment, and a general depletion of central carbon metabolites (succinate, citrate, glyceraldehyde 3-phosphate, ATP, MEP) in MMV228911-treated parasites. MMV595321 caused an accumulation of N-acetylated amino acids, and MMV688762 led to uracil deficiency and an accumulation of dihydroorotate and orotate. These data suggest that growth inhibitors cause a bipartite metabolic response composed of generic and compound-specific changes. While these findings highlight compound-specific metabolic signatures, some observed alterations may represent downstream or systemic effects of inhibitor action, reflecting the inherent complexity of parasite metabolism.

MMV1028806 and buparvaquone elicit metabolic responses similar to the *bc1*-complex inhibitor atovaquone

The metabolic impact of most tested MMV compounds indicated a novel mode of action that did not resemble known or recognizable metabolic fingerprints. However, the metabolic fingerprint of MMV1028806 was consistent with inhibition of pyrimidine biosynthesis at the bc_1-complex-dependent oxidation reaction of dihydroorotate to orotate, as has been reported for *P. falciparum* (Fig. 4A) (Allman et al. 2016; Creek et al. 2016; Antonova-Koch et al. 2018). A similar response would be expected to buparvaquone, which we found to be dually active against *T. gondii* tachyzoites and bradyzoites and which targets the bc_1-complex in *Theileria annulata* (McHardy et al. 1985), *Neospora caninum* (Müller et al. 2015) and *T. gondii* tachyzoites (Hayward et al. 2023).

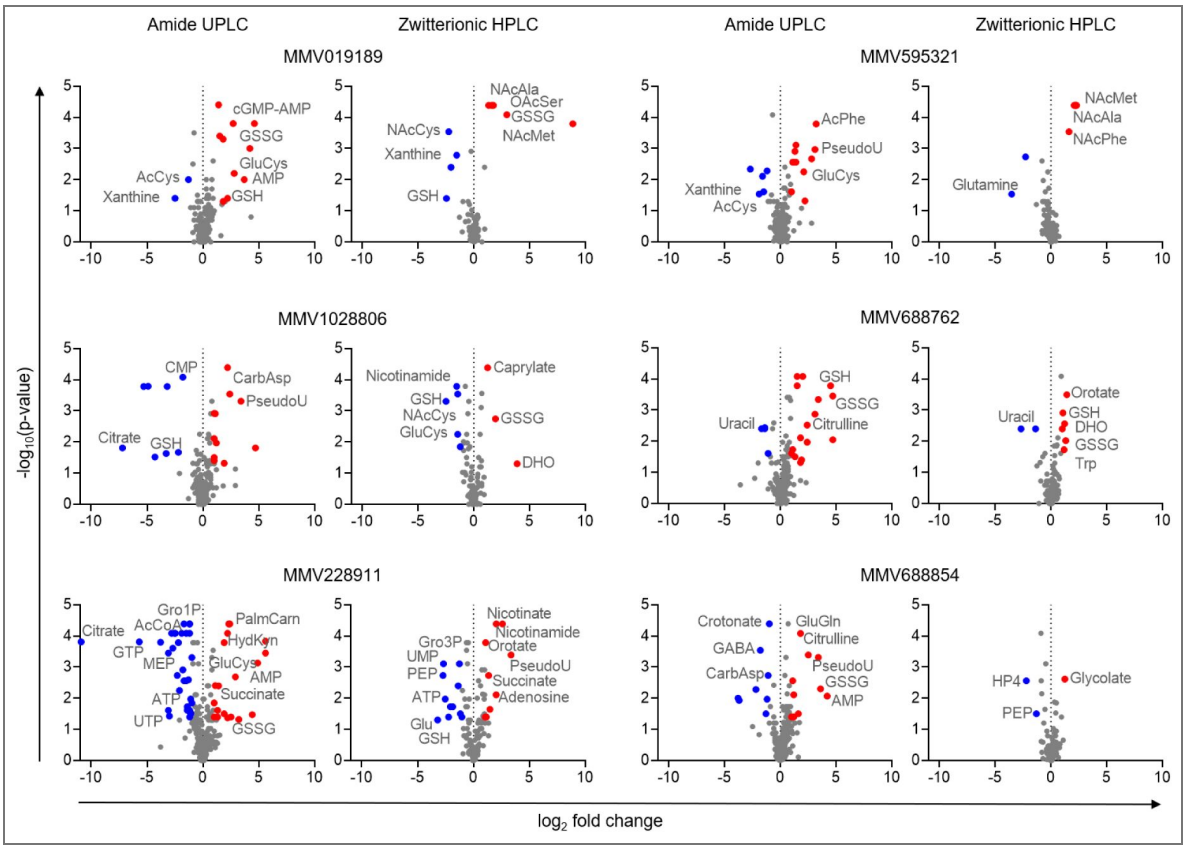

Figure 3. Untargeted metabolomics of tachyzoites treated with 6 screening hits effective against both stages of *T. gondii*.

Volcano plots showing the parasitic, intracellular metabolic phenotype caused by MMV Pathogen Box compounds that inhibited tachyzoites and bradyzoites during the screen. The metabolome was measured with two columns of complementary chemistries to enhance metabolite coverage. Blue dots indicate metabolites which were significantly reduced compared to DMSO treated parasites and red dots indicate significantly accumulated metabolites ($p < 0.05$, log2 fold change <-1 or > 1, 3x biological replicates with 3x technical replicates each, n = 9). Abbreviations: AcCoA - Acetyl-CoA, AcCys - Acetylcysteine, AcPhe - Acetylphenylalanine, AMP - Adenosinemonophosphate, ATP - Adenosinetriphosphate, CarbAsp - Carbamoylaspartate, cGMP-AMP - cyclic Guanosinemonophosphate-adenosinemonophosphate, CMP - Cytosinemonophosphate, DHO - Dihydroorotate, GABA - gamma-Aminobutyratic acid, GluCys - Glutamylcysteine, GluGln - Glutamylglutamine, Gro1P - Glyceraldehyde 1-phosphate, Gro3P - Glyceraldehyde 3-phosphate, GSH - Glutathione oxidized, GSSG - Glutathione reduced, GTP - Guanosinetriphosphate, HP4 - Hexose phosphate No 4 (fourth chromatographic peak of 260.02972), HydKyn - Hydroxylkynurenine, MEP - 2-C-Methyl-D-erythritol 4-phosphate, NAcAla - N-Acetylalanine, NAcCys - N-Acetylcysteine, NAcMet - N-Acetylmethionine, NAcPhe - N-Acetylphenylalanine, OAcSer - O-Acetylserine, PalmCarn - Palmitoylcarnitine, PEP - Phosphoenolpyruvate, PseudoU - Pseudouridine, Trp - Tryptophan, UMP - Uridinemonophosphate, UTP - Uridinetriphosphate

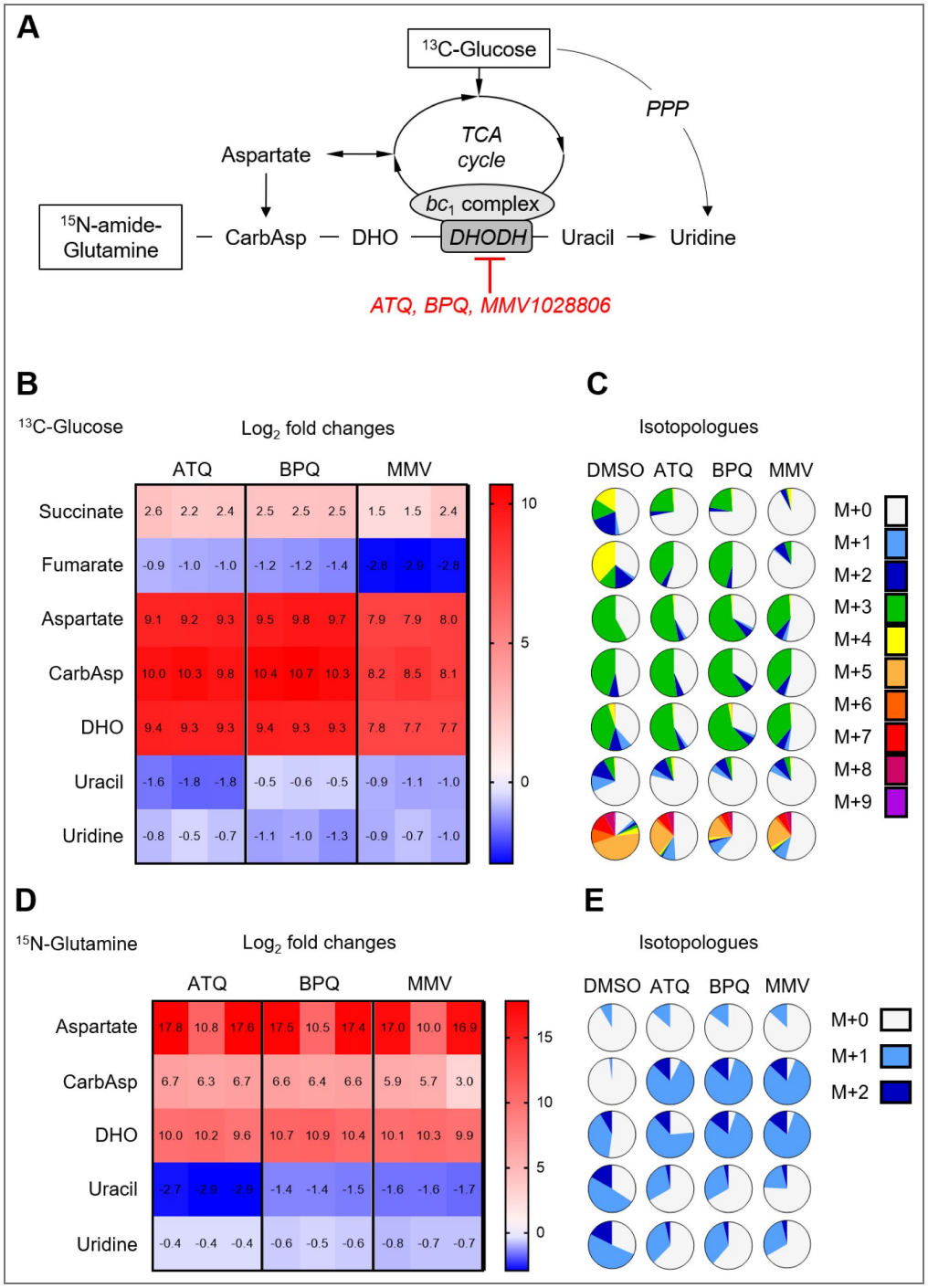

Figure 4. The metabolic response to electron transport chain inhibitors and MMV1028806.

(A) Scheme of the affected pathways upon bc_1-complex inhibition. Intracellular tachyzoites were grown in presence of U-^{13}C-glucose (B, C) or ^{15}N-amide-glutamine (D, E) instead of unlabeled carbon sources and treated with atovaquone (ATQ), buparvaquone (BPQ) and MMV1028806 (MMV) for 3h. (B, D) The treatment induced changes of mETC-related metabolite abundances are shown as $\log_2$-fold changes in comparison to DMSO treated cultures. Shown are three replicate measurements. (C, E) Shown is the average isotopologue distribution of mETC-related metabolites. The pie charts depict the number of heavy carbon or nitrogen atoms incooperated into the respective metabolites (M+0 in light grey represents the unlabeled metabolite, while M+1 in light blue indicates the intregation of one heavy atom into the molecule). Shown are the means of three replicate measurements. Abbreviations: ATQ - atovaquone, BPQ - buparvaquone, CarbAsp - carbamoyl-aspartate, DHO - dihydroorotate, DHODH - dihydroorotate dehydrogenase, GABA - gamma-aminobutyrate, MMV - MMV1028806, PPP - pentose phosphate pathway, SSA - succinic semialdehyde

To test these hypotheses, we exposed intracellular parasites to MMV1028806 or BPQ while substituting glucose with ^{13}C6-glucose for three hours. We then measured the incorporation of ^{13}C into the central carbon metabolites as well as the intermediates of the pyrimidine synthesis pathway. As controls, we utilized the known bc_1-complex inhibitor atovaquone and the solvent DMSO (Supplemental File 3). Treatment with all three inhibitors led to a dramatic accumulation of +3 labeled aspartic acid, carbamoyl aspartate and dihydroorotate which was accompanied by a depletion of uracil and uridine, in particular of the +5-labeled uridine isotopologue. These changes are consistent with impaired function of the bc_1-complex-dependent dihydroorotate dehydrogenase (Fig. 4B,C). Another common effect was the accumulation of succinate and depletion of fumarate, suggesting reduced recycling of $FADH_2$ via the bc_1-complex.

To independently verify our results, we hypothesized that *T. gondii* also incorporates glutamine-derived nitrogen into pyrimidines. We replaced glutamine with its ^{15}N-amide-labeled isotopologue in the tachyzoite culture media for three hours while simultaneously exposing the parasites to ATQ, BPQ or MMV1028806. As expected from our previous experiments, we observed a marked decrease of uracil and uridine levels while aspartate, carbamoyl aspartate and dihydroorotate accumulated again (Fig. 4D, Supplementary File 5). ^{15}N was incorporated into many metabolites (Fig. S4). Consistently, labelling of pyrimidines was diminished while carbamoyl aspartate and dihydroorotate were heavily labeled as M+1 isotopologues (Fig. 4E).

Together, these data show that treatments with all three compounds lead to the accumulation of metabolites upstream of the bc_1-complex-dependent reactions during pyrimidine biosynthesis and the TCA cycle and to the depletion of downstream metabolites (Fig. 4A). These metabolic signatures suggest an inhibition of the *T. gondii* bc_1-complex in tachyzoites.

Atovaquone, buparvaquone and MMV1028806 decrease the mitochondrial membrane potential of tachyzoites and bradyzoites and block the electron transport chain

The inhibition of the bc_1-complex by ATQ leads to the collapse of the mitochondrial membrane potential in *T. gondii* tachyzoites (Vercesi et al. 1998) and we anticipated a similar phenotype in BPQ or MMV1028806-treated parasites. We treated intracellular tachyzoites and bradyzoites for 24 h with the three inhibitors or 0.1 % DMSO alone and estimated the mitochondrial membrane potential and morphology using a fluorescent Mitotracker dye. The mitochondria of control tachyzoites appeared as extended loops but largely collapsed after treatments with all three compounds (Fig. 5A, B). Notably, also host mitochondria appear influenced. To evaluate the specificity of this assay we used pyrimethamine, clindamyin and 6-diazo-5-oxonorleucine (DON) that target dihydrofolate reductase, apicoplast translation and glutaminase as controls. Mitotracker and GFP signal intensities remained comparable to DMSO controls (Fig. S5). DAPI signal intensity appeared reduced in pyrimethamine-treated samples. In bradyzoites, mitochondria appeared mostly as spheres or were donut-shaped (Supplementary File 6) and their relative fluorescence decreased after 24 h treatment with ATQ, BPQ or MMV1028806 at 5 µM, 500 nM or 5 µM, respectively while their morphology appeared unchanged (Fig. 5C, D). Analysis by thin section electron microscopy revealed a largely unaffected sub-mitochondrial ultrastructure but the areas of mitochondrial profiles were changed in comparison to control after exposure with ATQ and MMV1028806 but not with BPQ (Fig. S6). This indicates that the latter decreases Mitotracker fluorescence intensity directly, while ATQ and MMV1028806 cause both, a drop in Mitotracker fluorescence and a reduced size of the mitochondria which leaves open whether a change of the membrane potential, of the size, or even of both parameters were responsible for the drop in Mitotracker fluorescence.

We next tested directly whether the mETC was blocked by ATQ, BPQ and MMV1028806 by measuring oxygen consumption of treated tachyzoites using a fluorescence-based assay (Fig. 5E). The solvent DMSO, the decoupling agent carbonyl cyanide 4-(trifluoromethoxy)phenylhydrazone (FCCP), and the *bc1*-complex inhibitor antimycin A served as controls. Treatment with FCCP led to a marked increase in oxygen consumption compared to the

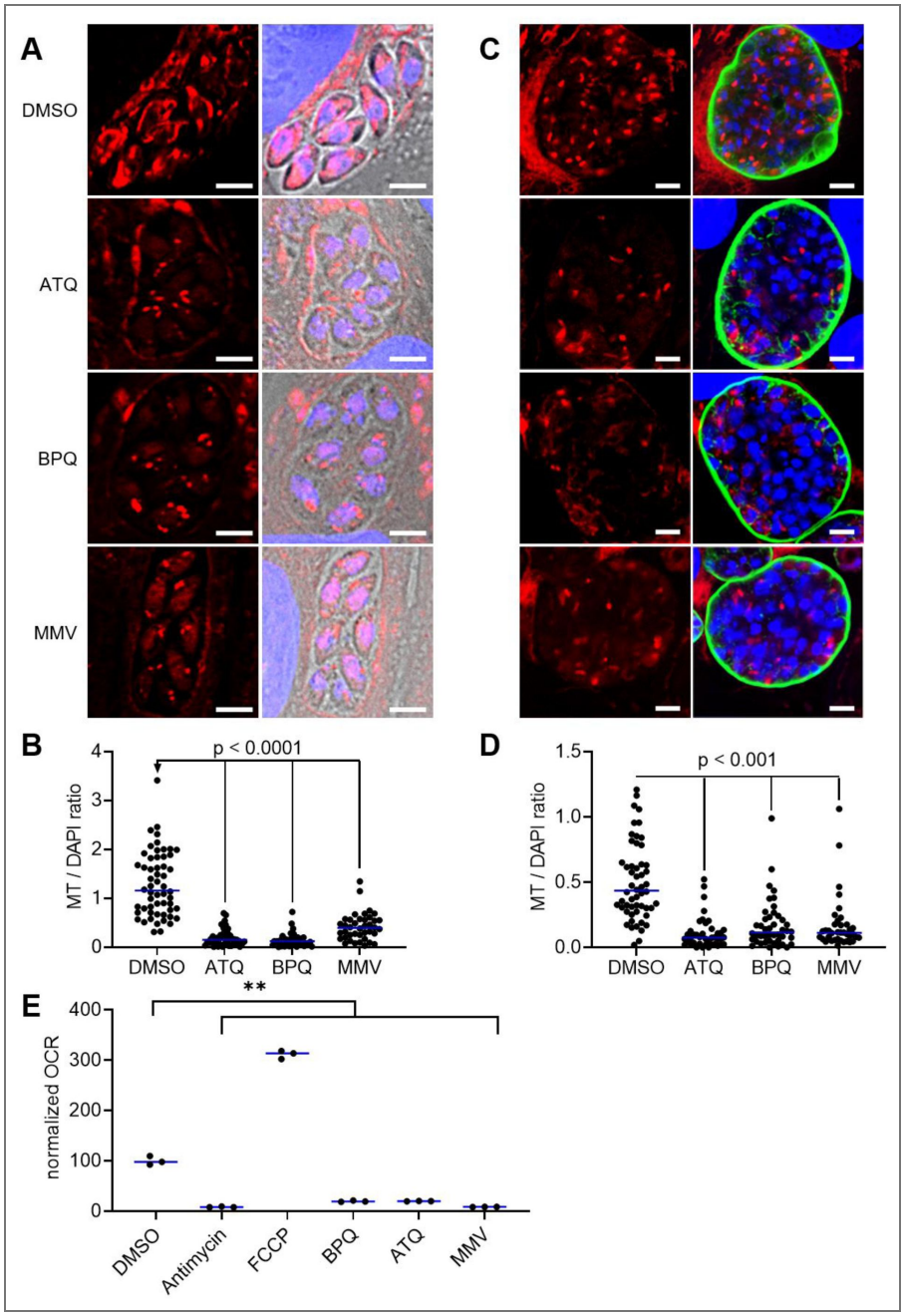

Figure 5. Atovaquone, buparvaquone, and MMV1028806 reduce mitochondrial potential and respiration in *T. gondii*.

(A) HFF cells were infected with tachyzoites and treated with DMSO, atovaquone, buparvaquone and MMV1028806 for 24 h, and mitochondria were stained with Mitotracker (red) and DNA was stained with DAPI (blue). scale bar = 5 µm. (B) The ratios of fluorescence intensities between mitotracker (MT) and DAPI dyes were calculated per vacuole (DMSO n = 56, ATQ n = 45, BPQ n = 49, MMV1028806 n = 40; Blue lines represent the median, two-sided Mann-Whitney test). (C) 4 weeks old, myotube derived ME49 in vitro cysts were treated with DMSO, atovaquone, buparvaquone and MMV1028806 for 24 h, and mitochondria were stained with mitotracker (red), the cyst wall was stained with Dolichos Biflorus Agglutinin and Streptavidin-Cy2 (green), and DNA was stained with DAPI (blue). scale bar = 20 µm. (D) The ratios of fluorescence intensities between mitotracker (MT) and DAPI dyes were calculated per vacuole (DMSO n = 56, ATQ n = 42, BPQ n = 45, MMV1028806 n = 38; Blue lines represent the median, two-sided Mann-Whitney test). (E) 10 million freshly egressed tachyzoites were incubated with known bc_1 complex inhibitors ATQ and BPQ, specific control compounds Antimycin and FCCP, and MMV1028806. Every treatment significantly impacts the oxygen consumption rate (OCR) (blue line represents the median, n = 3) (Welch's test; ** $p < 0.005$).

DMSO control, indicating maximal respiratory capacity of the parasites. In contrast, treatments with ATQ, BPQ, MMV1028806, and antimycin A resulted in substantially reduced oxygen consumption levels relative to the DMSO control and suggest indeed a blockage of the mETC consistent with the inhibition of the *bc1*-complex.

Inhibitors of the mitochondrial electron transport chain alter catabolic processes in bradyzoites

Next, we sought to confirm this mode of action directly on bradyzoites and record the metabolic impact of ATQ, BPQ or MMV1028806. To that end, we exposed intracellular four-week-old cysts to 5 µM, 500 nM or 5 µM of the respective compounds and for three hours and used 0.2% DMSO as a mock treatment. These concentrations represent their LC_{50} against bradyzoites and were chosen to minimize off-target effects. The cysts were isolated for LCMS analysis using magnetic beads (Christiansen et al. 2022) (Fig. 6A). Common in all three distinct metabolic phenotypes (Fig. S7) is the accumulation of AMP and NADH, while varying TCA cycle intermediates, such as malate, succinate and α-ketoglutarate and mitochondria-independent energy sources such as glucose and phosphocreatine were depleted (Fig. 6B-D). These metabolic changes suggest an energy starvation scenario marked by rising AMP levels and reduced recycling of NADH via the bc_1-complex. Interestingly, in BPQ and MMV1028806 treated cysts, we also observed prominent accumulation of several acyl-carnitines species which are mobile intermediates of ß-oxidation (Fig. 6B-D). Since this pathway is thought to be absent in *T. gondii,* we attribute these changes to inhibition of host mitochondria (Fig. 5A). Notably, we did not observe changes in the pyrimidine synthesis pathway, which may reflect low nucleic acid demand from largely dormant bradyzoites. These data demonstrate that bradyzoites, which were considered metabolically inactive, exhibit metabolic responses to inhibitory compounds. Although we characterized AMP accumulation as part of a general stress response in tachyzoites, the metabolic profiles of inhibited bradyzoites are consistent with inhibition of their mitochondrial bc_1-complex and suggest its role in ATP generation.

The differential efficacy of atovaquone and HDQ against bradyzoites correlates with the inhibition of ATP levels in bradyzoites

We sought to test the importance of the mETC chain in ATP generation in bradyzoites and exploited the differential targets of the coenzyme Q analogs ATQ and 1-hydroxy-2-dodecyl-4(1)quinolone (HDQ). However, while ATQ inhibits the bc_1-complex, HDQ inhibits dihydroorotate dehydrogenase (DHODH) (Hegewald, Gross, and Bohne 2013) and the alternative NADH dehydrogenase (NDH2) (Saleh et al. 2007). Both compounds block tachyzoite growth at low nanomolar concentrations in vitro with IC50s at 20 and 4 nM, respectively (Fig. 7A). However, in contrast to ATQ, HDQ does not affect the viability of mature *T. gondii* bradyzoites despite diminishing their mitochondrial membrane potential (Christiansen et al. 2022). Up to 20 µM HDQ did not arrest re-differentiation into proliferating tachyzoites, while bradyzoites that were treated with 5 µM ATQ (LC_{50} 2.5 µM) did not generate proliferating tachyzoites (Fig. 7B). To investigate how these modes of actions affect the mETC in bradyzoites, we tested their influence on mitochondrial ATP production by luciferase-based ATP assay. This assay shows a linear response to parasite cell equivalents between 10^3 and 10^6 parasites per 100 µL, and in order to minimize variance we decided to work with 10^5 parasites (Fig. S8). To maximize mitochondrial ATP production, we starved three-week-old bradyzoites for one additional week of glucose. As a comparison, we utilized tachyzoites that were cultured for two days in glucose-deplete conditions. Untreated tachyzoite samples contained in average 196 ± 21 fmol ATP per 10^5 parasites, whereas untreated bradyzoites only contained 14.1 ± 1.1 fmol. (Fig. 7C). Three hour-long treatment with 5 µM ATQ decreased ATP levels in both stages by 75 % (Fig. 7D). In contrast, HDQ reduced ATP levels by 60 % in tachyzoites but only marginally affected bradyzoites (Fig. 7D). These data

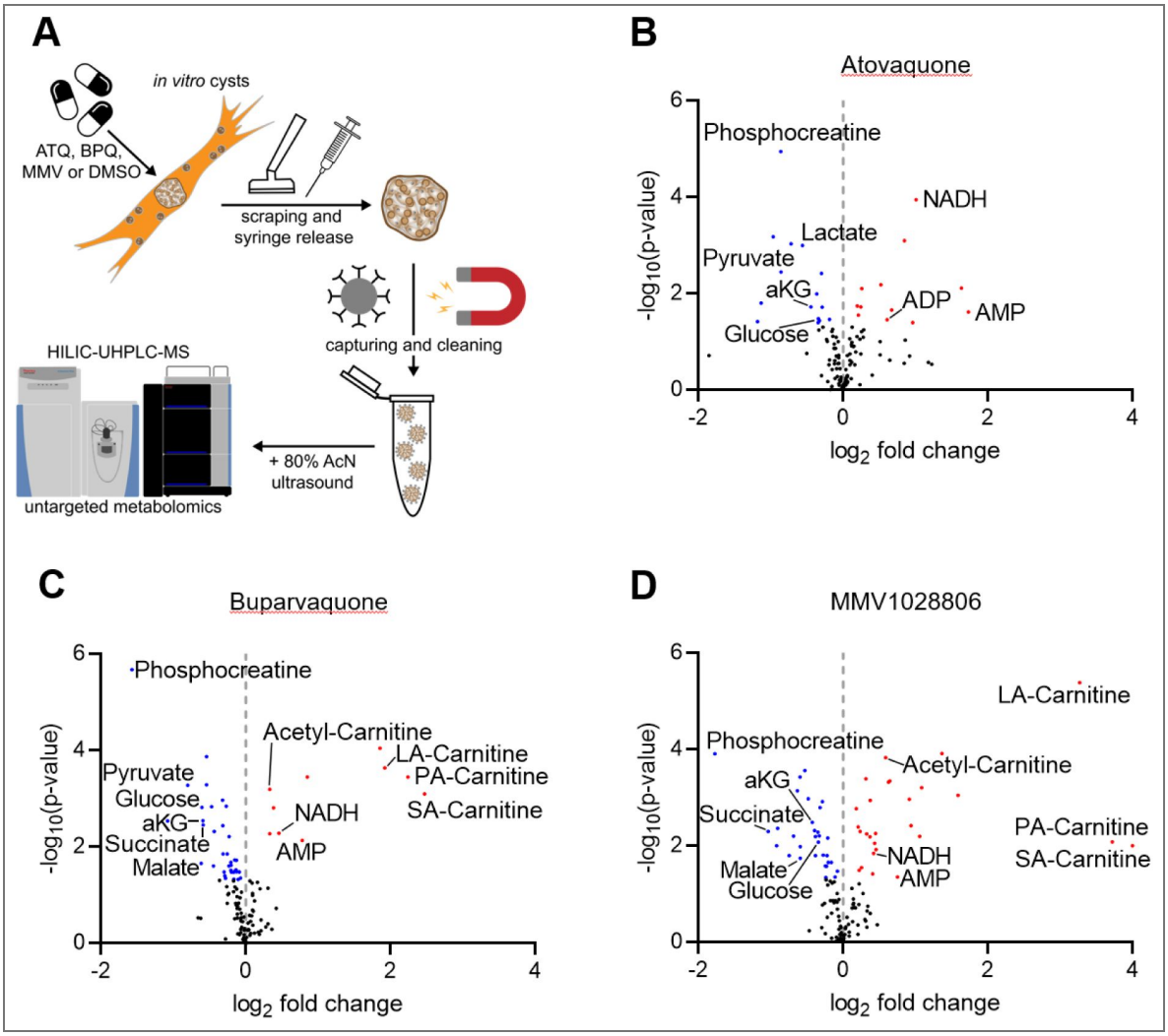

Figure 6. Untargeted metabolomic analysis of bradyzoites treated with bc_1-complex inhibitors shows an energy disbalance and hurdling mechanisms.

(A) Four weeks old *in vitro* cysts were treated for three hours. The cell monolayer was scraped off and the cysts were syringe-released. With Dolichos biflorus agglutinin (DBA) coated magnetic beads, the isolated cysts were captured and washed with PBS. The metabolites were extracted with 80% acetonitrile (AcN) in water and sonication, and analyzed via hydrophilic-interaction ultra-high pressure liquid chromatography coupled mass spectrometry (HILIC-UHPLC-MS). The results are shown in three separate volcano plots: Metabolic phenotypes of bradyzoites treated with Atovaquone (B), Buparvaquone (C), and MMV1028806 (D). (n = 3, significance analyzed with a two-sided U-Mann-Whitney test) Abbreviations: ATQ = atovaquone, BPQ = buparvaquone, DMSO = dimethylsulfoxide, LA-carnitine = linoleylcarnitine, MMV = MMV1028806, NADH = reduced nicotinamide adenine dinucleotide, PA-carnitine = palmitoylcarnitine, SA-carnitine = stearoylcarnitine

indicate that bradyzoites can maintain very low ATP levels and suggest the presence of a diminished but obligate production of ATP in the mitochondria that functions independently of exogenous glucose and HDQ-target enzymes.

Discussion

New treatment options for chronic *T. gondii* infections are needed, as chronic infections are currently incurable and available treatments for acute toxoplasmosis are associated with severe side-effects, in particular in infants after congenital transmission (Konstantinovic et al. 2019). To simultaneously identify drug targets in bradyzoites and along with their inhibitory compounds, we utilized a recently developed *in vitro* culture system of pan-drug tolerant bradyzoites (Christiansen et al. 2022) to screen 400 compounds of the MMV Pathogen Box. 16 compounds exhibited confirmed cidal activity against bradyzoites while also inhibiting growth of tachyzoites. Metabolic profiling and stable isotope tracing in treated tachyzoites suggested the inhibition of the mitochondrial bc_1-complex by MMV1028806 and the reference compound BPQ.

Interestingly, of the 15 compounds in the Toxoplasmosis disease set, previously earmarked by MMV, only 10 were found to be active against tachyzoites and none against bradyzoites. These differences may be attributed to strain-specific susceptibilities which are known for anti-folates and atovaquone (Meneceur et al. 2008) and differences in the design of growth assays. MMV assessed activities via plaque assays that prevent media change and rely on visual inspection of growth of a low number of parasites and might overestimate inhibitory effects.

We found that bradyzocidal compounds exhibit higher predicted logP coefficients, suggesting that the parasite entry might occur via diffusion across the cyst wall and less via solute transporter proteins. A known example of this principle is the anti-malarial drug fosmidomycin, where high polarity and low import rates caused minimal uptake by and efficacy against *T. gondii* tachyzoites (Nair et al. 2012; Baumeister et al. 2011). A similar case might also be made for the antifolates, pyrimethamine, sulfadiazine, trimethroprim and sulfamethoxazole which exhibit low consensus logP values of 2.09, 0.4, 1.16 and 0.92 and which also fail to eradicate tissue cysts (Alday and Doggett 2017; Enshaeieh et al. 2021). Interestingly, MMV675968 is a dually active compound with a logP value of 2.46, that has been shown to be a potent inhibitor of the dihydrofolate reductase (DHFR) in a range of pathogens (Songsungthong et al. 2019, 2021; Kim et al. 2021; Borba-Santos, Vila, and Rozental 2020; Nugraha et al. 2019; Rollin-Pinheiro et al. 2021; Vila and Lopez-Ribot 2017; Cantillon et al. 2022). Its target in *T. gondii*, however, remains to be identified.

Another important diffusion barrier that needs to be overcome to eradicate *T. gondii* tissue cysts is the blood brain barrier (BBB). Pyrimethamine and trimethroprim penetrate the blood brain barrier (Geils et al. 1971; Ineichen et al. 2020), they do not clear brain-resident cysts (Montazeri et al. 2018; Enshaeieh et al. 2021; Christiansen et al. 2022) highlighting the cyst wall as a potentially decisive obstacle. Consistent with this hypothesis is the tolerance of mature in vitro tissue cysts against high dose of sulfadiazine and pyrimethamine (Christiansen et al. 2022).

To characterize the modes of action of four additional inhibitors, we used metabolomics. In general, metabolic phenotypes reflect direct consequences of target inhibition as well as indirect effects resulting from attenuated growth and stress responses. We chose the bumped-kinase inhibitor MMV688854 (BKI-1294) that targets the calcium-dependent protein kinase 1 (CDPK1) as a control compound to identify metabolites implicated in a general stress response and adaptation to slow growth (Winzer et al. 2015). CDPK1 is needed for invasion (Johnson et al. 2012) and also affects formation of daughter cells. An accumulation of AMP and oxidized glutathione are the most conserved responses across the six treatments and may indicate depleted energy levels and oxidative stress (Caro et al. 2012). Also, pseudouridine is elevated in many treatments. Enhanced pseudouridylation of RNA is considered to be implicated in stress responses (Cerneckis et al. 2022) and modulates RNA stability (Davis 1995). It remains to be tested which of these conserved metabolic responses signify cellular decay and which ones take part in a productive metabolic response in *T. gondii*. Nonetheless, metabolic profiling data on antibiotics-exposed

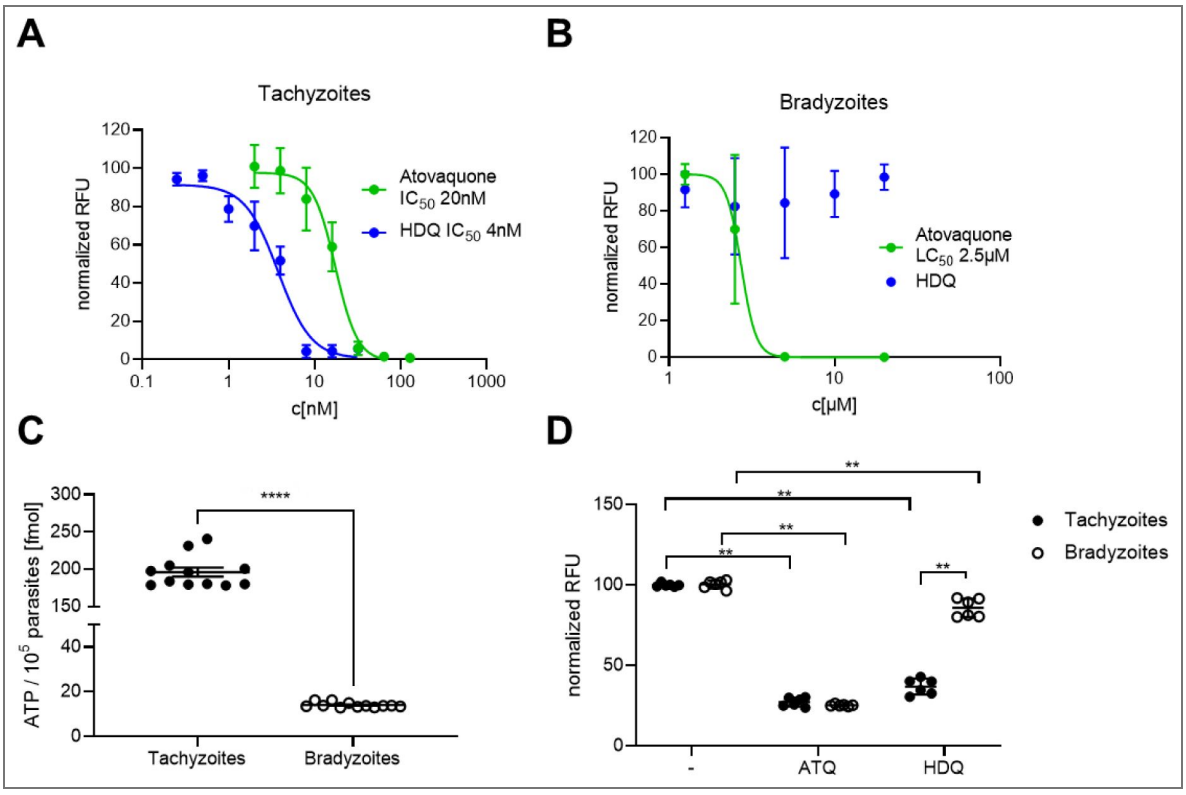

Figure 7. Differential efficacy and ATP depletion by atovaquone and HDQ in tachyzoites and bradyzoites.

Atovaquone and HDQ were tested against *T. gondii* Prugeniaud parasites. (A) Showing the normalized half-maximal inhibitory concentration (IC_{50}) against tachyzoites in fibroblasts at day 4, n=8. (B) 4-week-old bradyzoites were treated for a week with Atovaquone or HDQ. Cultures were observed for tachyzoite re-growth for three weeks. The half-maximal lethal concentration (LC_{50}) was determined at the time point which ideally reflected the dose-response curve, in this case day 14, n=6. 10^5 tachyzoites and bradyzoites were lysed and the ATP concentration was determined with an enzymatic luciferase assay. (C) Showing the calculated concentration of ATP within an average parasite. Lines reflect the median, error bars represent SEM, significance test Mann-Whitney, n=12. (D) Parasites were treated with 1µM Atovaquone or HDQ. RFUs were normalized to the untreated control of either the tachyzoite or bradyzoite dataset. Shown are means, error bars represent SD, significance test is pairwise Mann-Whitney, n=6.

bacterial pathogens has been used to design combination therapies, by either interfering with productive metabolic stress responses (Zampieri et al. 2017) or by simultaneously inhibiting otherwise non-essential pathways (Campos and Zampieri 2019). We found that the systematic identification of target structures and drug modes of action from profiling data alone remains challenging due to inherent non-linear relationships within the cellular metabolic network, the underlying regulatory mechanisms of enzyme functions. A systematic mapping of genetic disruptions to metabolic phenotypes, as demonstrated in *E. coli*, may alleviate these restrictions (Anglada-Girotto et al. 2022).

Apart from the general metabolic stress response to the treatment with MMV688854, three compounds caused apparent inhibitor-specific signatures. MMV019189, which is known to inhibit *P. falciparum* (Duffy et al. 2017), but also *C. parvum* (Hennessey et al. 2018) and *L. mexicana* (Berry et al. 2018), lead to the accumulation of c-GMP-AMP in the parasite. This dinucleotide is produced by the c-GMP-AMP synthase (cGAS) in mammalian cells in response to cytosolic DNA and triggers a type-I interferon response (Sun et al. 2013). While cGas is considered absent in *T. gondii*, host c-GMP-AMP induces STING-signaling as a response to *T. gondii* infection (P. Wang et al. 2019). Hence, MMV019189 may implicate the host in its antiparasitic activity.

MMV228911-treated tachyzoites showed the depletion of the DXR product 2-C-methylerythritol 4-phosphate (MEP), a metabolite that occurs in the non-mevalonate pathway in *T. gondii*'s apicoplast. Other metabolites upstream of DXR are either not detected or depleted, such as glyceraldehyde 3-phosphate, but also partake in other pathways. Interestingly, MMV228911 also caused a broader dysregulation of central carbon metabolism marked by a decrease of many phosphorylated metabolites such as nucleotide triphosphates and PEP but also citric acid and acetyl-CoA. This is consistent with metabolic signaling beyond the apicoplast, which also has been implicated in *P. falciparum*, where a cytosolic sugar phosphatase is responsible for resistance to the DXR inhibitor Fosmidomycin (Guggisberg et al. 2014).

We identified MMV1028806 as a candidate bc_1-complex inhibitor by comparing its metabolic impact with the one of BPQ with ATQ. All three compounds cause a sharp increase of pyrimidine synthesis substrates, depletion of pyrimidines and dysregulation of TCA cycle intermediates. This is consistent with previous mass spectrometry-based studies that characterized metabolic fingerprint of atovaquone on *P. falciparum* intraerythrocytic blood-stages (Creek et al. 2016; Allman et al. 2016; Antonova-Koch et al. 2018). Additionally, we confirmed the bc1-complex as a target by monitoring the incorporation of ^{13}C and ^{15}N stable isotopes from glucose and glutamine, respectively, into TCA cycle and pyrimidine biosynthesis intermediates. Both, the isotopologue distributions and metabolite abundances strongly suggest attenuation of pyrimidine production and TCA cycle fluxes by all three inhibitors (Hortua Triana et al. 2016). TCA cycle intermediates show characteristic isotopologue distributions that are indicative of a ^{13}C-label incorporation via acetyl-CoA (MacRae et al. 2012). A relatively increased M+3 isotopologue species in dicarboxylic acids in ATQ- and BPQ-treated parasites may indicate enhanced anaplerotic synthesis from glycolytic intermediates. These distinctions from MMV1028806 metabotypes may reflect a combination of off-target effects and differential timing of the metabolic inhibition.

Interestingly, six compounds from the MMV Pathogen Box have recently been shown to inhibit O_2 consumption in tachyzoites through bc_1-complex inhibition (Hayward et al. 2023). We co-identified Buparvaquone as a bc_1-complex inhibitor but we did not test the remaining five compounds for their targets. However, in our screen at 10 µM we found MMV024397 and MMV688853 to be dually active, while Trifloxystrobin (MMV688754) and Auranofin (MMV688978) lacked inhibitory activity in bradyzoites, and Azoxystrobin (MMV021057) was inactive. In addition, the previously described bc_1-complex inhibitor ELQ400 (MMV671636) (McConnell et al. 2018) was dually active. Overall, these data are consistent with the fact that the bc_1-complex is indeed needed for survival of bradyzoites, while not every tachyzocidal bc_1-inhibitor also inhibits bradyzoites.

In contrast to tachyzoites, the metabolic phenotype in bradyzoites is not dominated by dihydroorotate dehydrogenase (Fig. 6B, C, and D), as we observed neither the accumulation of carbamoyl-aspartate, dihydroorotate, and aspartate, nor the depletion of pyrimidines. Instead,

AMP and NADH accumulate, which in eukaryotes signifies a low cellular energy status (S.-C. Lin and Hardie 2018; X. Fu et al. 2019) that typically induces AMP-activated protein kinase and a glycolytic response. AMPK is a conserved enzyme with a pivotal role in cellular homeostasis: it responds to elevated AMP levels by repressing anabolic activity and by stimulating glucose uptake and glycolysis, β-oxidation, and ketogenesis (Winder and Hardie 1999; S.-C. Lin and Hardie 2018). *T. gondii* tachyzoites express AMPK which serves an important role in metabolic reprogramming during the lytic cycle of tachyzoites (Li et al. 2023). Transcriptomic and proteomic data indicate its presence in bradyzoites (Garfoot et al. 2019) but its function remains unknown. We observed decreased levels of free glucose during all three treatments that are consistent with stimulated glycolysis. We also observe depleted phosphocreatine levels in bradyzoites (Fig. 6) during treatments. In muscle cells, phosphocreatine acts as an ATP buffer system and replenishes ATP pools from ADP via creatine kinase (Kuby, Noda, and Lardy 1954; Perry 1954). It remains to be seen whether bradyzoites possess this mechanism. We also detect elevated levels of acyl-carnitines in BPQ and MMV1028806 treated bradyzoites. These molecules act as shuttles for the mitochondrial import of fatty acids for β-oxidation. However, this pathway has not been shown active and is deemed absent in *T. gondii* (Seeber, Limenitakis et al. 2008, Shunmugam, Arnold et al. 2022). The presence of acyl-carnitines in bradyzoites might reflect import from the host. It is conceivable that their elevation in response to buparvaquone and MMV1028806 indicates compromised functionality of the host bc_1-complex and subsequently accumulating β-oxidation substrates. Indeed, BPQ has a very broad activity across Apicomplexa (Hudson et al. 1985) and kinetoplastids (Croft et al. 1992).

We investigated the functionality of the mETC of tachyzoites and bradyzoites in response to ATQ, BPQ, and MMV1028806 by Mitotracker staining and thin section electron microscopy. All three treatments decrease overall Mitotracker fluorescence, consistent with a specific decrease mitochondrial electron potential (Supplementary Fig. 5). In contrast, pyrimethamine, clindamycin, and DON did not reduce the Mitotracker signal. Pyrimethamine-treated samples displayed an increased Mitotracker-to-DAPI ratio, which can be attributed to diminished DAPI intensity, likely resulting from inhibition of folate-dependent DNA synthesis via DHFR blockade. Clin-treated samples showed no change in mitochondrial morphology or ratio, in line with its delayed-death phenotype. Similarly, DON, which targets glutamine metabolism, did not alter mitochondrial signal or ratio at 24 hours, though morphological changes were observed. Together, these findings confirm that disruption of mitochondrial membrane potential is specific to compounds targeting the electron transport chain, while inhibitors acting on nuclear or metabolic pathways do not induce rapid mitochondrial dysfunction under the conditions tested. ATQ and MMV1028806 but not BPQ also shrink areas of mitochondrial cross-sections indicating a potential contribution to the observed change in overall fluorescence. These differences might reflect distinct mitochondrial morphologies. In agreement with previous observations (Place et al. 2023), we found that bradyzoite mitochondria differ from those in tachyzoites, predominantly occurring as “blobs” rather than tubes or loops, and our observations align with these findings (Supplementary File 6).

The oxygen consumption assays highlight the functional sensitivity of the T. gondii RHku80 mETC to pharmacological perturbation (Fig. 5E). As expected, FCCP, an uncoupler of oxidative phosphorylation, markedly increased oxygen consumption, confirming the parasite’s ability to upregulate electron flow when the proton gradient is dissipated. Antimycin A nearly abolished respiration, demonstrating the essential role of complex III in maintaining mitochondrial activity. Likewise, ATQ and BPQ, both *bc1*-complex inhibitors, strongly suppressed oxygen consumption. Notably, MMV1028806 produced a comparable inhibitory effect, suggesting that it also targets complex III or a functionally linked site within the mitochondrial electron transport chain. This observation differs from the findings of (Hayward et al. 2023), who did not report MMV1028806 as an mETC inhibitor in their Seahorse-based screen of the MMV Pathogen Box. A key difference is that our assays were performed at 10 μM, whereas (Hayward et al. 2023) used 1 μM. These results support a mitochondrial mode of action for MMV1028806 under our experimental conditions and underline the value of oxygen consumption assays for detecting dose-dependent effects on parasite respiration.

Our findings strongly suggest that bradyzoite survival is critically dependent on mitochondrial electron transport. We investigated this by comparing the effects of two inhibitors: HDQ, which kills tachyzoites but not bradyzoites, and ATQ, which kills both. Although HDQ enters bradyzoites and reduces their mitochondrial membrane potential, its inability to kill them implies its molecular targets are non-essential in this stage. To pinpoint the vital process, we measured ATP levels and found that only the bradyzocidal compound, ATQ, caused a collapse in bradyzoite ATP. HDQ did not, despite both drugs depleting ATP in tachyzoites. This directly links bradyzoite viability to mitochondrial ATP production. The different outcomes are explained by their distinct targets: ATQ inhibits the *bc1*-complex (McFadden et al. 2000), which is central to ATP synthesis, whereas HDQ blocks other pathways like pyrimidine synthesis and mitochondrial NADH oxidation through DHODH and NDH2. These results also support the notion that the canonical TCA cycle is not the primary source of electrons for bradyzoites (Christiansen et al. 2022). A variety of electron sources supply the electron transport chain (Maclean et al. 2021). The sources that are crucial for ATP production remain to be identified.

Bradyzoites may also utilize glycolysis to generate ATP. This has been suggested to be the case in early, seven-day-old bradyzoites where gliding motility, an ATP dependent process, can be inhibited by withdrawal of exogenous glucose and by the glycolytic inhibitor 2-deoxyglucose. However, in these parasites, also Oligomycin A inhibited motility suggesting an simultaneously essential contribution of the mitochondrial ATP (Fu, Brown et al. 2021). In addition, hexokinase has been shown to be needed for optimal cyst production in chronically infected mice, suggesting an important role of this protein either though its enzymatic activity or other functions (Shukla et al. 2018). It remains to be investigated how mature bradyzoites rely on glycolysis to produce ATP and how this is integrated with mitochondrial ATP production.

Interestingly, despite its profound effect on ATP levels and viability of bradyzoites, ATQ fails to eradicate all *T. gondii* cysts from infected mice and does not reliably prevent toxoplasmosis relapse in AIDS patients and mice (Araujo, Huskinson, and Remington 1991; Kovacs 1992; Ferguson et al. 1994; Katlama, Mouthon, et al. 1996). Underlying reasons for this discrepancy need to be established but may include insufficient bioavailability. Quinolones are known to be poorly soluble in aqueous environments. In addition, the predicted permeability of the blood-brain barriers to either ATQ, BPQ and HDQ is low. Indeed, improved bioavailability of ATQ in nanosuspensions improved efficacies (Shubar et al. 2011). Also, BPQ treatment of mice that were experimentally infected with closely related *Neospora caninum* parasites did target parasites in muscle but not in brain tissue (Müller et al. 2015). A similar conjecture arose when comparing endochin-like quinolones. Here, favorable pharmacokinetics of a variant with lower intrinsic potency likely conferred higher *in vivo* efficacy against cysts (Doggett et al. 2012).

Together, our data illustrate the functional importance of the bc_1-complex for the viability of bradyzoites and encourage the pursuit of bc_1-complex inhibitors as candidates for curative toxoplasmosis treatment. Both, efforts to develop multi-site-directed inhibitors (Doggett et al. 2020; Alday, Nilsen, and Doggett 2022) and re-purposing of respective drugs are promising avenues. However, our data also underline the importance of favorable pharmacokinetics to ensure passage through the blood-brain barrier and the cyst wall.

Data availability

Metabolomic data been deposited at *ftp://massive-ftp.ucsd.edu/v11/MSV000100157/* and are poublicly available.

Supplementary figures

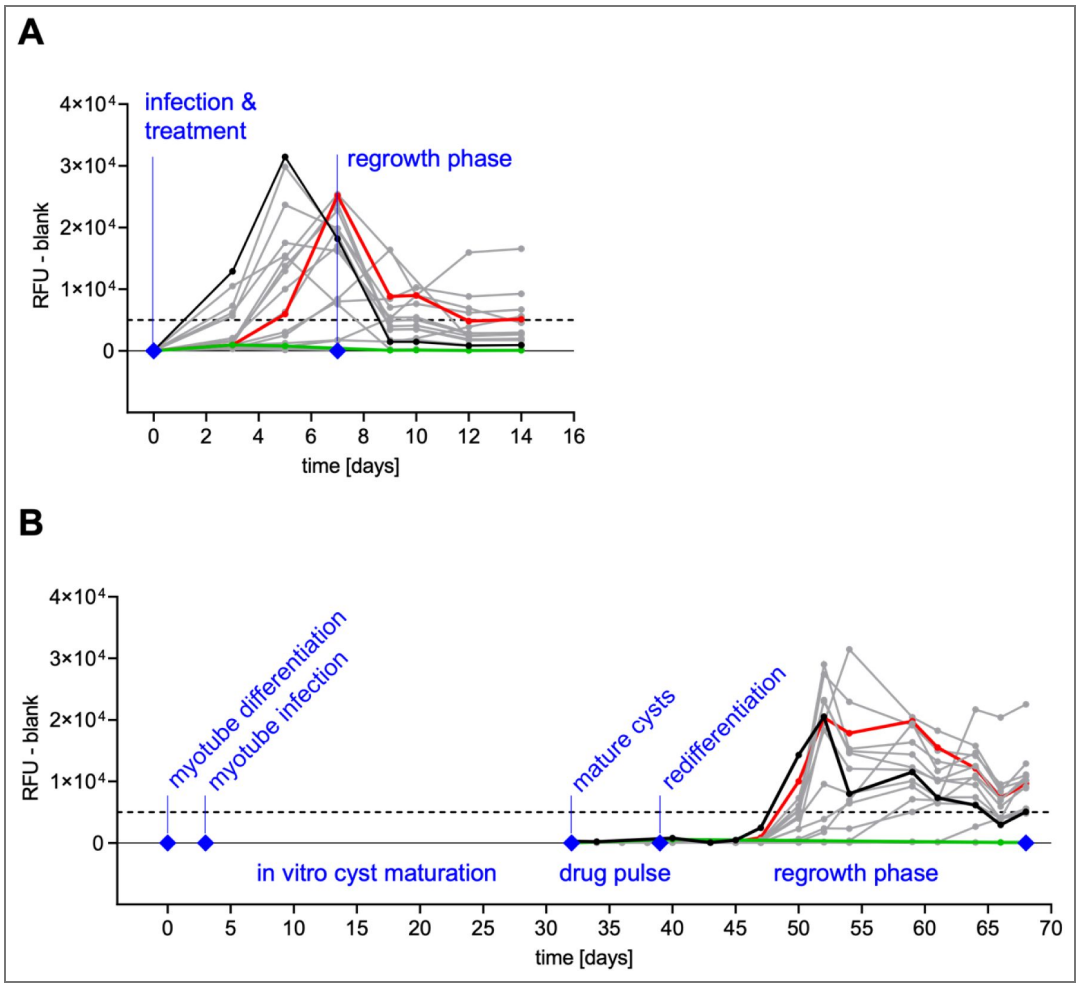

Figure S1. Longitudinal Screening Procedure All 400 compounds of the MMV Pathogen Box were screened against (A) tachyzoites (n = 4) and (B) in vitro tissue cysts (n = 3). Plotted fluorescence values were background-subtracted and reflect the abundance of parasites per treatment over time (black line = solvent control, green line = inhibitory compound, red line = ineffective compound, dashed line = growth threshold).

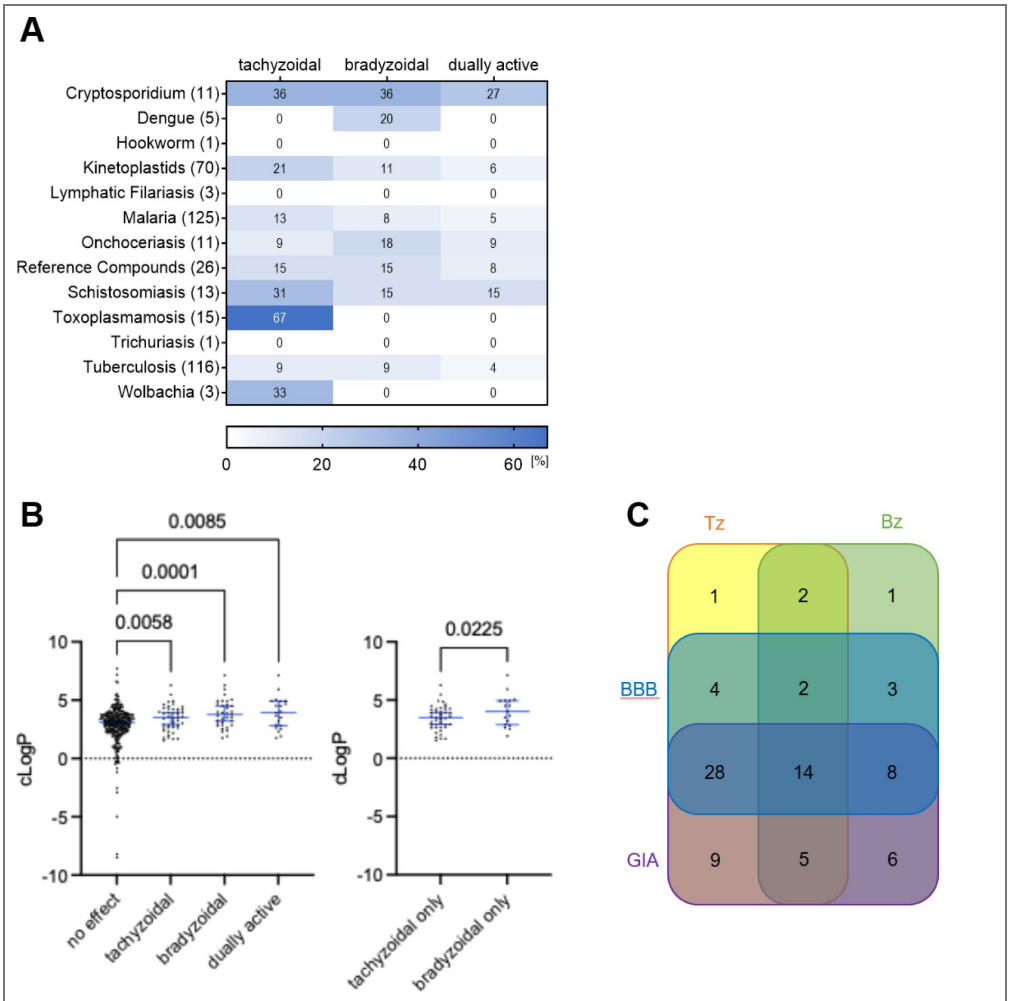

D

Compound	Tachyzoite IC_{50} [µM] Mean ± SEM	Tachyzoite lowest cytotoxity [µM]	Bradyzoite LC_{50} [µM] Mean ± SEM	Bradyzoite lowest cytotoxity [µM]
MMV011765	0.14 ± 0.05	5	0.8 ± 0.2	
MMV019189	0.28 ± 0.04		2.7 ± 0.8	
MMV021013	0.28 ± 0.05	10	1.4 ± 0.3	10
MMV022478	1 ± 0.2	5	2.79 ± 0.07	
MMV595321	0.28 ± 0.01		1.3 ± 0.2	
MMV658988	0.28 ± 0.01		3.4 ± 0.2	
MMV659004	0.25 ± 0.02		2.4 ± 0.2	10
MMV671636 (ELQ-400)	0.0059 ±0.0006		0.42 ± 0.04	
MMV675968	0.00105 ± 0.00007		0.9 ± 0.2	
MMV676477	0.034 ± 0.005	0.3	0.53 ± 0.07	5
MMV687807	0.01 ± 0.003	0.08	0.71 ± 0.01	2.5
MMV688762	1.1 ± 0.1		8.2 ± 0.9	
MMV688853	0.061 ± 0.009		1.8 ± 0.2	
MMV688854 (BKI-1294)	0.191 ± 0.007		3.6 ± 0.3	
MMV689480 (BPQ)	0.00007 ± 0.00006		0.15 ± 0.03	
MMV1028806	0.98 ± 0.07		4.4 ± 0.3	

Figure S2. Properties of dually active screening hits.

(A) Table showing the relative amount of tachyzocidal, bradyzocidal and dually-active compounds per originally indicated target species. E.g. 11 compounds were indicated by MMV to be active against Cryptosporidium and 36% and 27% of these are bradyzocidal and dually active, whereas 67% of the 15 compounds indicated as active against Toxoplasmosis possessed activity against tachyzoites but none was active against against bradyzoites. (B) Estimated lipophilicity approximated by predicted partition coefficient suggest that active compounds generally exhibit an increased lipophilicity compared to inactive compounds. (C) A Venn diagram showing intersections of tachy- and bradyzocidal compounds as well as their predicted gastrointestinal absorption capability (GIA) and blood brain barrier (bbb) permeability. (D) Tabulation of compound IC_{50} and LC_{50} data of confirmed active compounds. The calculated IC_{50}s and LC_{50}s of 16 dually active compounds from figure 2 are summarized in this table. The tachyzoite IC_{50}s represent 8 replicates, the bradyzocidal one where generated from 6 replicates. Lowest cytotoxicity values were recorded during the primary screen as detailed in the methods section.

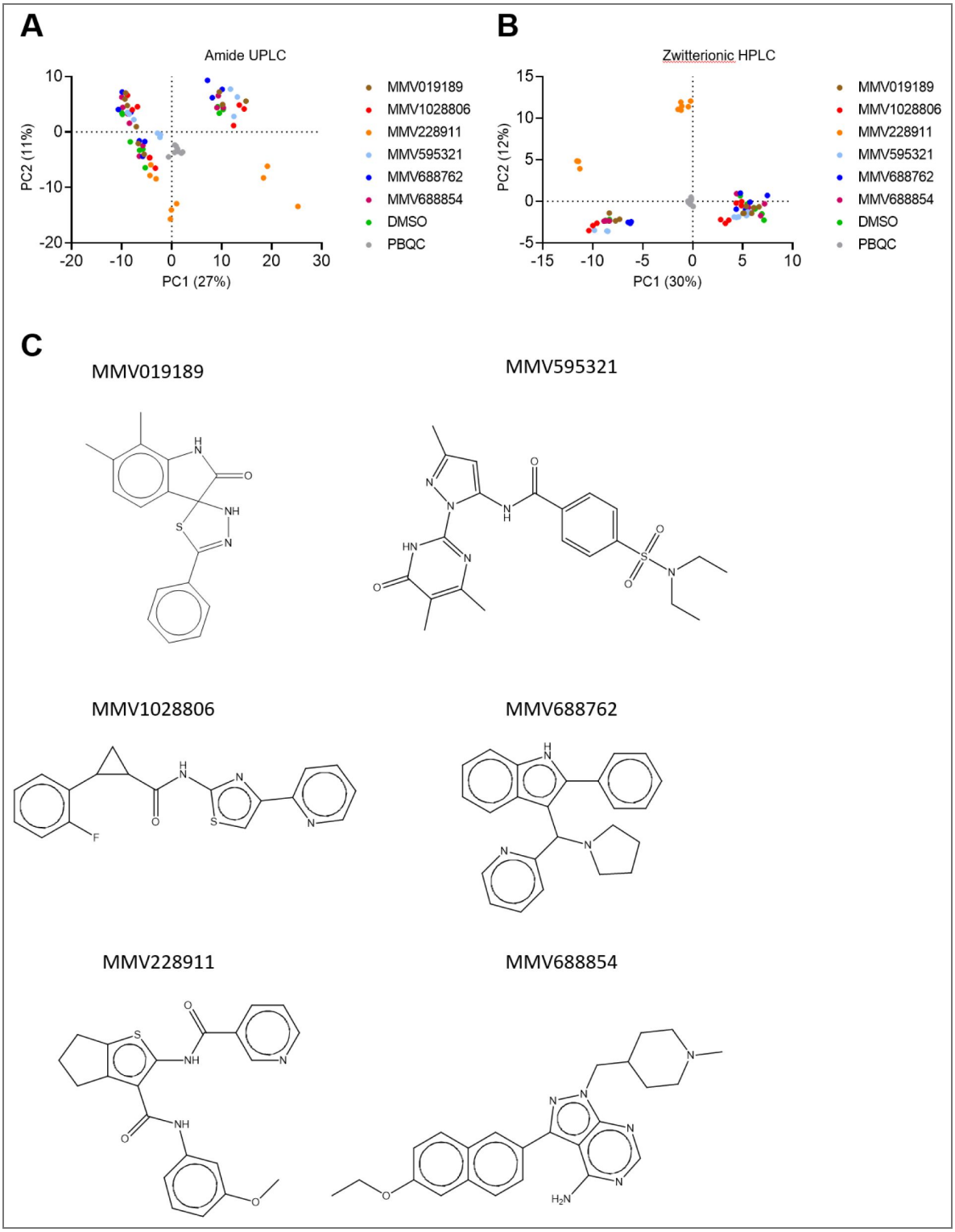

Figure S3. Principal component analysis of LCMS metabolomes of treated parasites using two chromatographic colums.

(A) Principal component analysis of metabolites from extracellular tachyzoites that were treated with indicated MMV compounds. Metabolites were separated using BEH-Amide column -HILIC chromatography and detected by mass spectrometry. (B) The same metabolite extracts have been re-analysed using pHILIC-column HILIC chromatography for separation instead. (C) Chemical structures of dually active and tested compounds as provided by MMV.

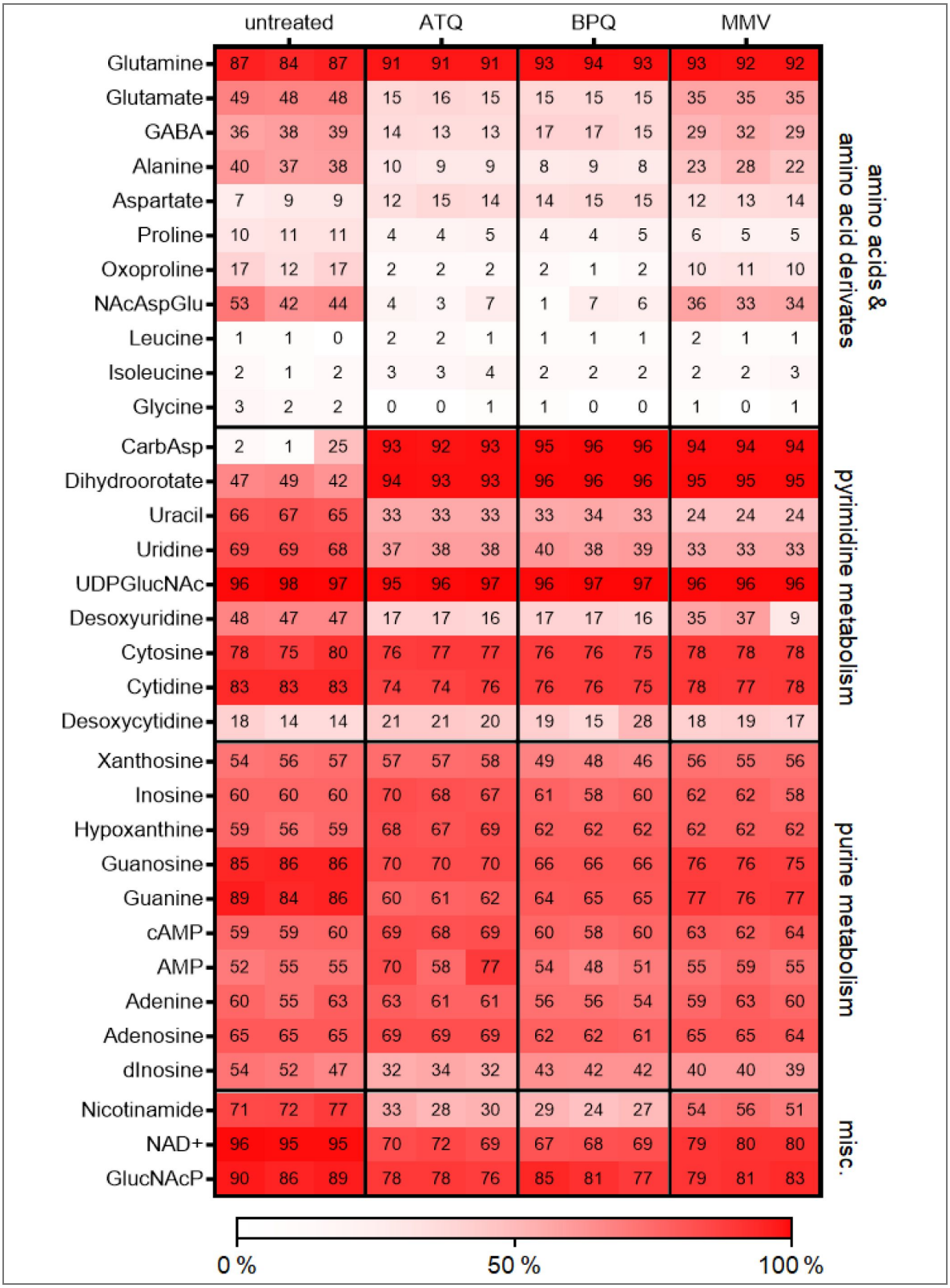

Figure S4. Intracellular tachyzoites exhibit differential ^{15}N incorporation after treatment with mETC inhibitors.

RH-KU80 were treated with atovaquone, buparvaquone and MMV1028806, labeled with ^{15}N-amide-L-glutamine for 3h, followed by their isolation from the HFF cells. The heatmap shows the overall isotopic labeling (100-"M+0") of each replicate.

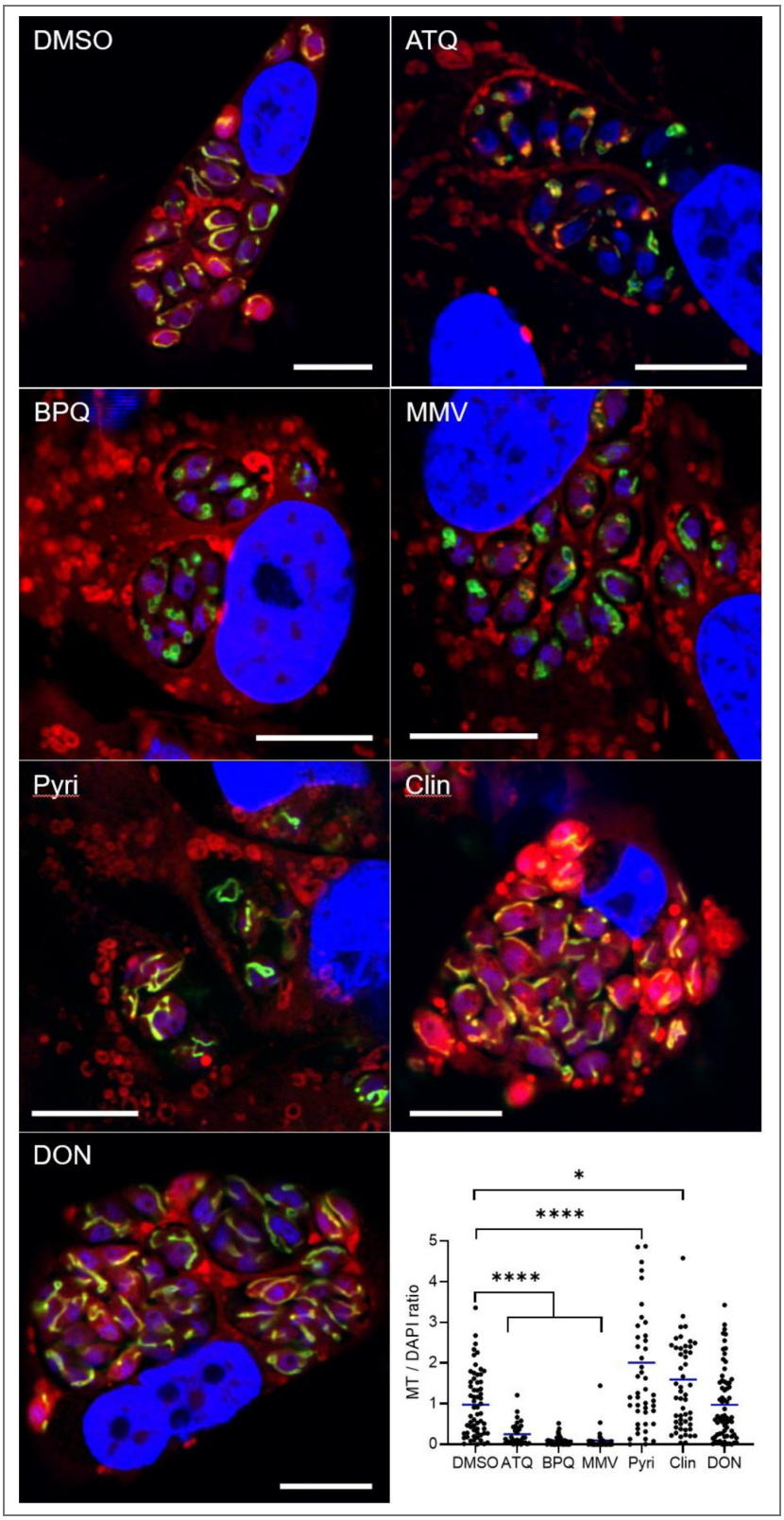

Figure S5. Direct mitochondrial inhibitors reduce Mitotracker signal intensity and MT/DAPI ratio in *T. gondii* tachyzoites.

HFF cells were infected with RH-S9 tachyzoites and treated for 24h with DMSO, atovaquone (ATQ), buparvaquone (BPQ), MMV1028806 (MMV), pyrimethamine (Pyri), clindamycin (Clin), and 6-Diazo-5-oxonorleucine (DON). * and **** denote $p < 0.05$ and $p < 0.000$ in Mann-Whitney tests).

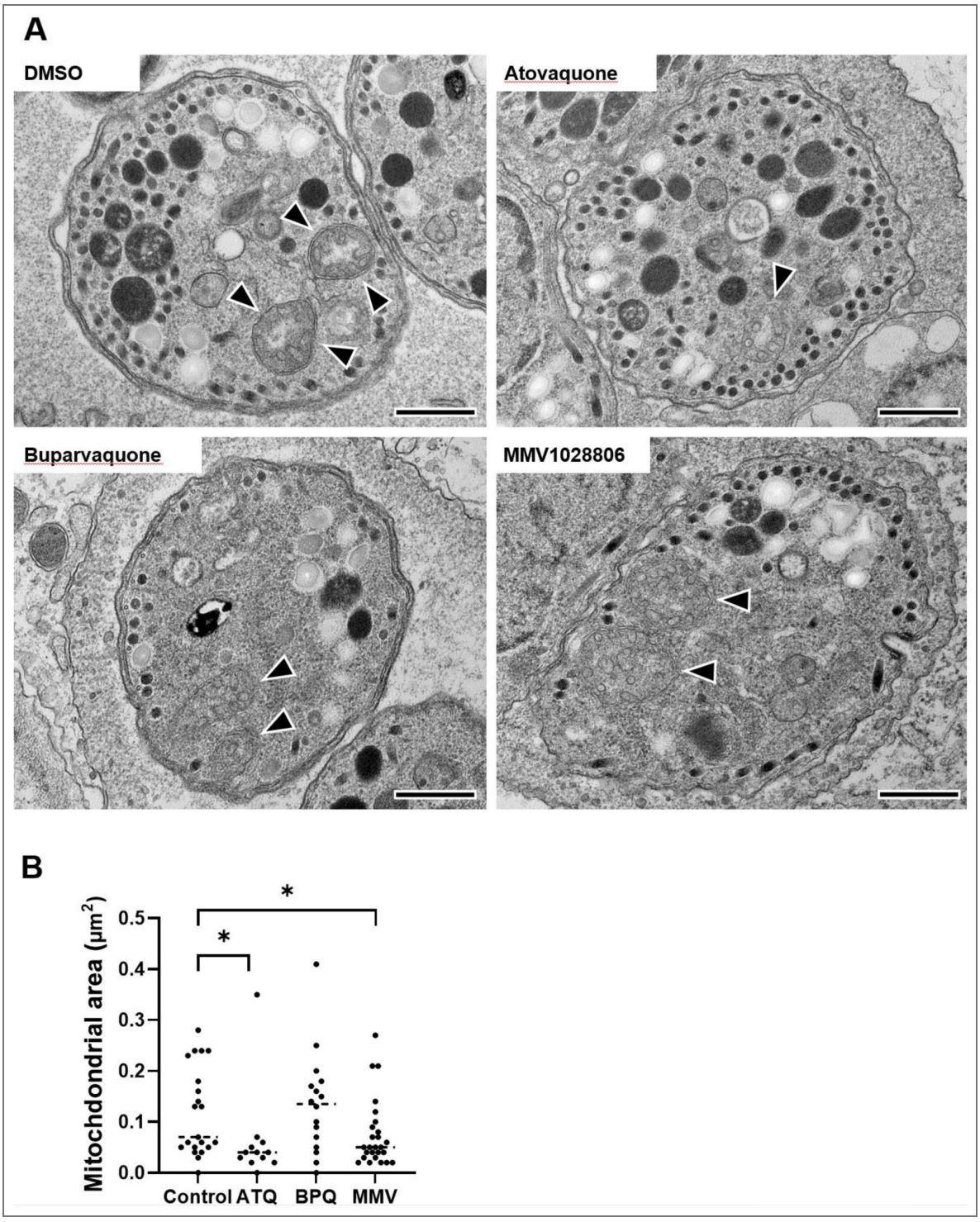

Figure S6. ***bc*$_1$-complex inhibitors partially reduce mitochondrial profiles of bradyzoites.**

Thin section electron microscopy of cysts that were treated with atovaquone (ATQ), buparvaquone (BPQ) or MMV1028806 (MMV) for 24 h (A). (B) Measured areas of mitochondrial profiles from 21, 12, 15 and 26 images showing DMSO, ATQ, BPQ and MMV1028806 treated parasites (* denotes $p < 0.05$ in Mann-Whitney tests). Mitotracker signal appears red, DAPI stain is blue, and the mitochondrial signal originates from GFP. Scale bars represent 10µm. The graph is showing the ratio of the Mitotracker to DAPI signal intensity within each individual parasitophorous vacuole (DMSO n = 61, ATQ n = 32, BPQ n = 35, MMV1028806 n = 36; Pyri n = 58, Clin n = 53, DON n = 68. Blue lines represent the median, two-sided Mann-Whitney test).

Figure S7. Principal component analysis of bradyzoites treated with atovaquone (ATQ), Buparvaquone (BPQ) and MMV1028806.

Four-week-old intracellular cysts were exposed for three hours, purified from their host cells using magnetic beads and analyzed by LCMS.

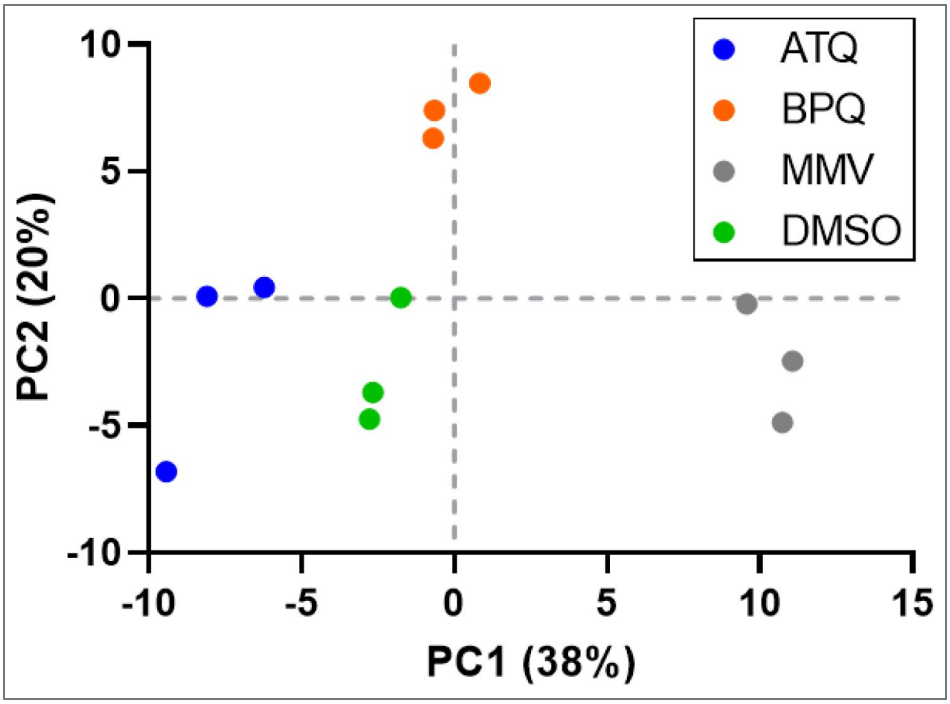

Figure S8. Luminescence-based ATP assay

(A) The linear response of the BacTiter-Glo™ assay has a certain range, depending on the ATP concentration of the sample. The assay is reliable between 100 fM and 1 nM ATP. (B) Increasing numbers of freshly isolated parasites were analysed to determine a minimal parasite density necessary for steady readouts. 10^5 parasites per sample were both manageable and accurate.

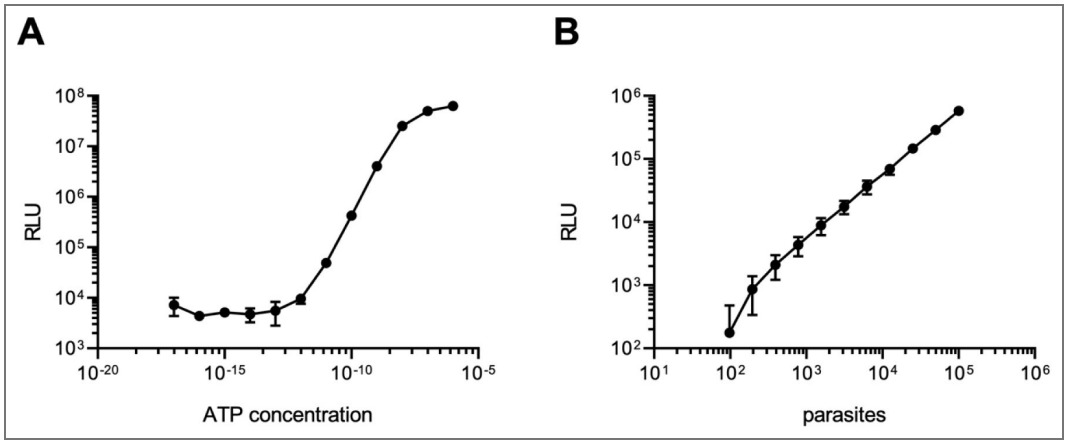

Acknowledgements

We thank Naohiro Hashimoto for sharing the KD3 cells and the Medicine for Malaria Venture for the Pathogen Box and Silvio Bürge for his imaging support. MB, DM, EP are funded by the Federal Ministry of Education and Research (BMBF) under project number 01KI1715 as part of the "Research Network Zoonotic Infectious Diseases". MB, DM, FS, TH, ML are funded by the Robert Koch Institute.

Additional files

Supplemental File 1
Supplemental File 2
Supplemental File 3
Supplemental File 4
Supplemental File 5
Supplemental File 6

Additional information

Funding

Funder	Grant reference number	Author
Federal Ministry of Education and Research (BMBF)	01KI1715	Deborah Maus Elyzana Putrianti Martin Blume
Robert Koch Institut (RKI)		Deborah Maus Tobias Hoffmann Frank Seeber Michael Laue Martin Blume

Author ORCID iDs

Deborah Maus: https://orcid.org/0000-0002-9688-2663
Tobias Hoffmann: https://orcid.org/0000-0003-2858-4776
Michael Laue: https://orcid.org/0000-0002-6474-9139
Frank Seeber: https://orcid.org/0000-0002-2271-3699
Martin Blume: https://orcid.org/0000-0002-6894-3000

References

Alday P. Holland, Doggett Joseph Stone (2017) Drugs in Development for Toxoplasmosis: Advances, Challenges, and Current Status. *Drug Design, Development and Therapy* **11**:273-93

Alday P. Holland, Nilsen Aaron, Doggett J. S. (2022) Structure-Activity Relationships of Toxoplasma Gondii Cytochrome Bc1 Inhibitors. *Expert Opinion on Drug Discovery* **17**:997-1011

Allman Erik L., Painter Heather J., Samra Jasmeet, Carrasquilla Manuela, Llinás Manuel (2016) Metabolomic Profiling of the Malaria Box Reveals Antimalarial Target Pathways. *Antimicrobial Agents and Chemotherapy* **60**:6635-49

Anglada-Girotto Miquel, Handschin Gabriel, Ortmayr Karin, Campos Adrian I., Gillet Ludovic, Manfredi Pablo, Mulholland Claire V., et al. (2022) Combining CRISPRi and Metabolomics for Functional Annotation of Compound Libraries. *Nature Chemical Biology* **18**:482-91

Antonova-Koch Yevgeniya, Meister Stephan, Abraham Matthew, Luth Madeline R., Ottilie Sabine, Lukens Amanda K., Sakata-Kato Tomoyo, et al. (2018) Open-Source Discovery of Chemical Leads for next-Generation Chemoprotective Antimalarials. *Science* **362**
https://doi.org/10.1126/science.aat9446

Araujo F. G., Huskinson J., Remington J. S. (1991) Remarkable in Vitro and in Vivo Activities of the Hydroxynaphthoquinone 566C80 against Tachyzoites and Tissue Cysts of Toxoplasma Gondii. *Antimicrobial Agents and Chemotherapy* **35**:293-99

Bajohr Lara Liv, Ma Ling, Platte Christian, Liesenfeld Oliver, Tietze Lutz F., Gross Uwe, Bohne Wolfgang (2010) In Vitro and in Vivo Activities of 1-Hydroxy-2-Alkyl-4(1H)Quinolone Derivatives against Toxoplasma Gondii. *Antimicrobial Agents and Chemotherapy* **54**:517-21

Baumeister Stefan, Wiesner Jochen, Reichenberg Armin, Hintz Martin, Bietz Sven, Harb Omar S., Roos David S., et al. (2011) Fosmidomycin Uptake into Plasmodium and Babesia-Infected Erythrocytes Is Facilitated by Parasite-Induced New Permeability Pathways. *PloS One* **6**:e19334

Berry Sarah L., Hameed Hamza, Thomason Anna, Maciej-Hulme Marissa L., Abou-Akkada Somaia Saif, Horrocks Paul, Price Helen P. (2018) Development of NanoLuc-PEST Expressing Leishmania Mexicana as a New Drug Discovery Tool for Axenic-and Intramacrophage-Based Assays. *PLoS Neglected Tropical Diseases* **12**:e0006639

Borba-Santos Luana Pereira, Vila Taissa, Rozental Sonia (2020) Identification of Two Potential Inhibitors of Sporothrix Brasiliensis and Sporothrix Schenckii in the Pathogen Box Collection. *PloS One* **15**:e0240658

Campos Adrian I., Zampieri Mattia (2019) Metabolomics-Driven Exploration of the Chemical Drug Space to Predict Combination Antimicrobial Therapies. *Molecular Cell* **74**:1291-1303.

Cantillon Daire, Goff Aaron, Taylor Stuart, Salehi Emad, Fidler Katy, Stoneham Simon, Waddell Simon J. (2022) Searching for New Therapeutic Options for the Uncommon Pathogen Mycobacterium Chimaera: An Open Drug Discovery Approach. *The Lancet Microbe* **3**:e382-91

Caro Pilar, Kishan Amar U., Norberg Erik, Stanley Illana A., Chapuy Bjoern, Ficarro Scott B., Polak Klaudia, et al. (2012) Metabolic Signatures Uncover Distinct Targets in Molecular Subsets of Diffuse Large B Cell Lymphoma. *Cancer Cell* **22**:547-60

Cerneckis Jonas, Cui Qi, He Chuan, Yi Chengqi, Shi Yanhong (2022) Decoding Pseudouridine: An Emerging Target for Therapeutic Development. *Trends in Pharmacological Sciences* **43**:522-35

Christiansen Céline, Maus Deborah, Hoppenz Ellen, Murillo-León Mateo, Hoffmann Tobias, Scholz Jana, Melerowicz Florian, Steinfeldt Tobias, Seeber Frank, Blume Martin (2022) In Vitro Maturation of Toxoplasma Gondii Bradyzoites in Human Myotubes and Their Metabolomic Characterization. *Nature Communications* **13**:1168

Creek Darren J., Chua Hwa H., Cobbold Simon A., Nijagal Brunda, MacRae James I., Dickerman Benjamin K., Gilson Paul R., Ralph Stuart A., McConville Malcolm J. (2016) Metabolomics-Based Screening of the Malaria Box Reveals Both Novel and Established Mechanisms of Action. *Antimicrobial Agents and Chemotherapy* **60**:6650-63

Croft S. L., Hogg J., Gutteridge W. E., Hudson A. T., Randall A. W. (1992) The Activity of Hydroxynaphthoquinones against Leishmania Donovani. *The Journal of Antimicrobial Chemotherapy* **30**:827-32

Daina Antoine, Michielin Olivier, Zoete Vincent (2017) Scientific Reports. pp. 42717

Davis D. R (1995) Stabilization of RNA Stacking by Pseudouridine. *Nucleic Acids Research* **23**:5020-26

DeRocher A., Hagen C. B., Froehlich J. E., Feagin J. E., Parsons M. (2000) Analysis of Targeting Sequences Demonstrates That Trafficking to the Toxoplasma Gondii Plastid Branches off the Secretory System. *Journal of Cell Science* **113**:3969-77

Doggett J. Stone, Nilsen Aaron, Forquer Isaac, Wegmann Keith W., Jones-Brando Lorraine, Yolken Robert H., Bordón Claudia, et al. (2012) Endochin-like Quinolones Are Highly Efficacious against Acute and Latent Experimental Toxoplasmosis. *Proceedings of the National Academy of Sciences of the United*

States of America **109**:15936-41

Doggett J. Stone, Ojo Kayode K., Fan Erkang, Maly Dustin J., Van Voorhis Wesley C. (2014) Bumped Kinase Inhibitor 1294 Treats Established Toxoplasma Gondii Infection. *Antimicrobial Agents and Chemotherapy* **58**:3547-49

Doggett J. Stone, Schultz Tracey, Miller Alyssa J., Bruzual Igor, Pou Sovitj, Winter Rolf, Dodean Rozalia, et al. (2020) Orally Bioavailable Endochin-Like Quinolone Carbonate Ester Prodrug Reduces Toxoplasma Gondii Brain Cysts. *Antimicrobial Agents and Chemotherapy* **64** https://doi.org/10.1128/AAC.00535-20

Duffy Sandra, Sykes Melissa L., Jones Amy J., Shelper Todd B., Simpson Moana, Lang Rebecca, Poulsen Sally-Ann, Sleebs Brad E., Avery Vicky M. (2017) Screening the Medicines for Malaria Venture Pathogen Box across Multiple Pathogens Reclassifies Starting Points for Open-Source Drug Discovery. *Antimicrobial Agents and Chemotherapy* **61** https://doi.org/10.1128/AAC.00379-17

Enshaeieh Marjan, Saadatnia Geita, Babaie Jalal, Golkar Majid, Choopani Samira, Sayyah Mohammad (2021) Valproic Acid Inhibits Chronic Toxoplasma Infection and Associated Brain Inflammation in Mice. *Antimicrobial Agents and Chemotherapy* **65**:e0100321

Ferguson D. J., Huskinson-Mark J., Araujo F. G., Remington J. S. (1994) An Ultrastructural Study of the Effect of Treatment with Atovaquone in Brains of Mice Chronically Infected with the ME49 Strain of Toxoplasma Gondii. *International Journal of Experimental Pathology* **75**:111-16

Fu Xiaorong, Deja Stanisław, Kucejova Blanka, Duarte Joao A. G., McDonald Jeffrey G., Burgess Shawn C. (2019) Targeted Determination of Tissue Energy Status by LC-MS/MS. *Analytical Chemistry* **91**:5881-87

Fu Yong, Brown Kevin M., Jones Nathaniel G., Moreno Silvia Nj, David Sibley L. (2021) Toxoplasma Bradyzoites Exhibit Physiological Plasticity of Calcium and Energy Stores Controlling Motility and Egress. *eLife* **10**:December https://doi.org/10.7554/eLife.73011

Garfoot Andrew L., Wilson Gary M., Coon Joshua J., Knoll Laura J. (2019) Proteomic and Transcriptomic Analyses of Early and Late-Chronic Toxoplasma Gondii Infection Shows Novel and Stage Specific Transcripts. *BMC Genomics* **20**:859

Geils G. F., Scott Jr C. W., Baugh C. M. (1971) Treatment of Meningeal Leukemia with Pyrimethamine. *Blood* **38**:131-37

Guggisberg Ann M., Park Jooyoung, Edwards Rachel L., Kelly Megan L., Hodge Dana M., Tolia Niraj H., Odom Audrey R. (2014) A Sugar Phosphatase Regulates the Methylerythritol Phosphate (MEP) Pathway in Malaria Parasites. *Nature Communications* **5**:4467

Havelaar Arie H., Kirk Martyn D., Torgerson Paul R., Gibb Herman J., Hald Tine, Lake Robin J., Praet Nicolas, et al. (2015) World Health Organization Global Estimates and Regional Comparisons of the Burden of Foodborne Disease in 2010. *PLoS Medicine* **12**:e1001923

Hayward Jenni A., Victor Makota F., Cihalova Daniela, Leonard Rachel A., Rajendran Esther, Zwahlen Soraya M., Shuttleworth Laura, et al. (2023) A Screen of Drug-like Molecules Identifies Chemically Diverse Electron Transport Chain Inhibitors in Apicomplexan Parasites. *PLoS Pathogens* **19**:e1011517

Hegewald Jana, Gross Uwe, Bohne Wolfgang (2013) Identification of Dihydroorotate Dehydrogenase as a Relevant Drug Target for 1-Hydroxyquinolones in Toxoplasma Gondii. *Molecular and Biochemical Parasitology* **190**:6-15

Hennessey Kelly M., Rogiers Ilse C., Shih Han-Wei, Hulverson Matthew A., Choi Ryan, McCloskey Molly C., Whitman Grant R., et al. (2018) Screening of the Pathogen Box for Inhibitors with Dual Efficacy against Giardia Lamblia and Cryptosporidium Parvum. *PLoS Neglected Tropical Diseases* **12**:e0006673

Triana Hortua, Andrea Miryam, Herrera Daniela Cajiao, Zimmermann Barbara H., Fox Barbara A., Bzik David J. (2016) Pyrimidine Pathway-Dependent and -Independent Functions of the Toxoplasma Gondii Mitochondrial Dihydroorotate Dehydrogenase. *Infection and Immunity* **84**:2974-81

Hudson A. T., Randall A. W., Fry M., Ginger C. D., Hill B., Latter V. S., McHardy N., Williams R. B. (1985) Novel Anti-Malarial Hydroxynaphthoquinones with Potent Broad Spectrum Anti-Protozoal Activity. *Parasitology* **90**:45-55

Hulverson Matthew A., Bruzual Igor, McConnell Erin V., Huang Wenlin, Vidadala Rama S. R., Choi Ryan, Arnold Samuel L. M., et al. (2019) Pharmacokinetics and In Vivo Efficacy of Pyrazolopyrimidine, Pyrrolopyrimidine, and 5-Aminopyrazole-4-Carboxamide Bumped Kinase Inhibitors against Toxoplasmosis. *The Journal of Infectious Diseases* **219**:1464-73

Ineichen Benjamin V., Di Palma Serena, Laczko Endre, Liddelow Shane A., Neumann Susanne, Schwab Martin E., Mosberger Alice C. (2020) Regional Differences in Penetration of the Protein Stabilizer Trimethoprim (TMP) in the Rat Central Nervous System. *Frontiers in Molecular Neuroscience* **13**:167

John Beena, Harris Tajie H., Tait Elia D., Wilson Emma H., Gregg Beth, Ng Lai Guan, Mrass Paulus, et al. (2009) Dynamic Imaging of CD8+ T Cells and Dendritic Cells during Infection with Toxoplasma Gondii. *PLoS Pathogens* **5**:e1000505

Johnson Steven M., Murphy Ryan C., Geiger Jennifer A., DeRocher Amy E., Zhang Zhongsheng, Ojo Kayode K., Larson Eric T., et al. (2012) Development of Toxoplasma Gondii Calcium-Dependent Protein Kinase 1 (TgCDPK1) Inhibitors with Potent Anti-Toxoplasma Activity. *Journal of Medicinal Chemistry* **55**:2416-26

Katlama C., De Wit S., O'Doherty E., Van Glabeke M., Clumeck N. (1996) Pyrimethamine-Clindamycin vs. Pyrimethamine-Sulfadiazine as Acute and Long-Term Therapy for Toxoplasmic Encephalitis in Patients with AIDS. *Clinical Infectious Diseases: An Official Publication of the Infectious Diseases Society of America* **22**:268-75

Katlama C., Mouthon B., Gourdon D., Lapierre D., Rousseau F. (1996) Atovaquone as Long-Term Suppressive Therapy for Toxoplasmic Encephalitis in Patients with AIDS and Multiple Drug Intolerance. Atovaquone Expanded Access Group. *Aids* **10**:1107-12

Kim Haeun, Burkinshaw Brianne J., Lam Linh G., Manera Kevin, Dong Tao G. (2021) Identification of Small Molecule Inhibitors of the Pathogen Box against Vibrio Cholerae. *Microbiology Spectrum* **9**:e0073921

Konstantinovic Neda, Guegan Hélène, Stäjner Tijana, Belaz Sorya, Robert-Gangneux Florence (2019) Treatment of Toxoplasmosis: Current Options and Future Perspectives. *Food and Waterborne Parasitology* **15**:e00036

Kovacs J. A (1992) Efficacy of Atovaquone in Treatment of Toxoplasmosis in Patients with AIDS. *The Lancet* **340**:637-38

Kuby S. A., Noda L., Lardy H. A. (1954) Adenosinetriphosphate-Creatine Transphosphorylase. I. Isolation of the Crystalline Enzyme from Rabbit Muscle. *The Journal of Biological Chemistry* **209**:191-201

Laue Michael (2010) Electron Microscopy of Viruses. *Methods in Cell Biology* **96**:1-20

Li Yaqiong, Niu Zhipeng, Yang Jichao, Yang Xuke, Chen Yukun, Li Yingying, Liang Xiaohan, et al. (2023) Rapid Metabolic Reprogramming Mediated by the AMP-Activated Protein Kinase during the Lytic Cycle of Toxoplasma Gondii. *Nature Communications* **14**:422

Lin Sheng-Cai, Grahame Hardie D. (2018) AMPK: Sensing Glucose as Well as Cellular Energy Status. *Cell Metabolism* **27**:299-313

Maclean Andrew E., Bridges Hannah R., Silva Mariana F., Ding Shujing, Ovciarikova Jana, Hirst Judy, Sheiner Lilach (2021) Complexome Profile of Toxoplasma Gondii Mitochondria Identifies Divergent Subunits of Respiratory Chain Complexes Including New Subunits of Cytochrome Bc1 Complex. *PLoS Pathogens* **17**:e1009301

MacRae James I., Sheiner Lilach, Nahid Amsha, Tonkin Christopher, Striepen Boris, McConville Malcolm J. (2012) Mitochondrial Metabolism of Glucose and Glutamine Is Required for Intracellular Growth of Toxoplasma Gondii. *Cell Host & Microbe* **12**:682-92

Maus Deborah, Curtis Blake, Warschkau David, Betancourt Estefanía Delgado, Seeber Frank, Blume Martin (2024) Generation of Mature Toxoplasma Gondii Bradyzoites in Human Immortalized Myogenic KD3 Cells. *Bio-Protocol* **14**:e4916

McConnell Erin V., Bruzual Igor, Pou Sovitj, Winter Rolf, Dodean Rozalia A., Smilkstein Martin J., Krollenbrock Alina, et al. (2018) Targeted Structure-Activity Analysis of Endochin-like Quinolones Reveals Potent Qi and Qo Site Inhibitors of Toxoplasma Gondii and Plasmodium Falciparum Cytochrome Bc1 and Identifies ELQ-400 as a Remarkably Effective Compound against Acute Experimental Toxoplasmosis. *ACS Infectious Diseases* **4**:1574-84

McFadden D. C., Tomavo S., Berry E. A., Boothroyd J. C. (2000) Characterization of Cytochrome b from Toxoplasma Gondii and Q(o) Domain Mutations as a Mechanism of Atovaquone-Resistance. *Molecular and Biochemical Parasitology* **108**:1-12

McHardy N., Wekesa L. S., Hudson A. T., Randall A. W. (1985) Antitheilerial Activity of BW720C (Buparvaquone): A Comparison with Parvaquone. *Research in Veterinary Science* **39**:29-33

Meneceur Pascale, Bouldouyre Marie-Anne, Aubert Dominique, Villena Isabelle, Menotti Jean, Sauvage Virginie, Garin Jean-François, Derouin Francis (2008) In Vitro Susceptibility of Various Genotypic Strains of Toxoplasma Gondii to Pyrimethamine, Sulfadiazine, and Atovaquone. *Antimicrobial Agents and Chemotherapy* **52**:1269-77

Metsalu Tauno, Vilo Jaak (2015) ClustVis: A Web Tool for Visualizing Clustering of Multivariate Data Using Principal Component Analysis and Heatmap. *Nucleic Acids Research* **43**:W566-70

Montazeri Mahbobeh, Mehrzadi Saeed, Sharif Mehdi, Sarvi Shahabeddin, Shahdin Shayesteh, Daryani Ahmad (2018) Activities of Anti-Toxoplasma Drugs and Compounds against Tissue Cysts in the Last Three Decades (1987 to 2017), a Systematic Review. *Parasitology Research* **117**:3045-57

Montazeri Mahbobeh, Galeh Tahereh Mikaeili, Moosazadeh Mahmood, Sarvi Shahabeddin, Dodangeh Samira, Javidnia Javad, Sharif Mehdi, Daryani Ahmad (2020) The Global Serological Prevalence of Toxoplasma Gondii in Felids during the Last Five Decades (1967-2017): A Systematic Review and Meta-Analysis. *Parasites & Vectors* **13**:82

Montoya J. G., Liesenfeld O. (2004) Toxoplasmosis. *The Lancet* **363**:1965-76

Müller Joachim, Aguado-Martinez Adriana, Manser Vera, Balmer Vreni, Winzer Pablo, Ritler Dominic, Hostettler Isabel, Arranz-Solís David, Ortega-Mora Luis, Hemphill Andrew (2015) Buparvaquone Is Active against Neospora Caninum in Vitro and in Experimentally Infected Mice. *International Journal for Parasitology, Drugs and Drug Resistance* **5**:16-25

Nair Sethu C., Brooks Carrie F., Goodman Christopher D., Sturm Angelika, McFadden Geoffrey I., Sundriyal Sandeep, Anglin Justin L., Song Yongcheng, Moreno Silvia N. J., Striepen Boris (2012) Apicoplast Isoprenoid Precursor Synthesis and the Molecular Basis of Fosmidomycin Resistance in Toxoplasma Gondii. *The Journal of Experimental Medicine* **209**:1051-1051

Nixon G. L., Moss D. M., Shone A. E., Lalloo D. G., Fisher N. (2013) O, Neill, PM; Ward, SA; Biagini, GA. *The Journal of Antimicrobial Chemotherapy*

Nugraha Arifin Budiman, Tuvshintulga Bumduuren, Guswanto Azirwan, Tayebwa Dickson Stuart, Rizk Mohamed Abdo, Gantuya Sambuu, Batiha Gaber El-Saber, et al. (2019) Screening the Medicines for Malaria Venture Pathogen Box against Piroplasm Parasites. *International Journal for Parasitology, Drugs and Drug Resistance* **10**:84-90

Pan Ming, Ge Ceng-Ceng, Fan Yi-Min, Jin Qi-Wang, Shen Bang, Huang Si-Yang (2022) The Determinants Regulating Toxoplasma Gondii Bradyzoite Development. *Frontiers in Microbiology* **13**:1027073

Perry S. V (1954) Creatine Phosphokinase and the Enzymic and Contractile Properties of the Isolated Myofibril. *Biochemical Journal* **57**:427-34

Rollin-Pinheiro Rodrigo, Borba-Santos Luana Pereira, da Silva Xisto Mariana Ingrid Dutra, de Castro-Almeida Yuri, Rochetti Victor Pereira, Rozental Sonia, Barreto-Bergter Eliana (2021) Identification of Promising Antifungal Drugs against Scedosporium and Lomentospora Species after Screening of Pathogen Box Library. *Journal of Fungi (Basel, Switzerland)* **7** https://doi.org/10.3390/jof7100803

Saleh Ahmad, Friesen Johannes, Baumeister Stefan, Gross Uwe, Bohne Wolfgang (2007) Growth Inhibition of Toxoplasma Gondii and Plasmodium Falciparum by Nanomolar Concentrations of 1-Hydroxy-2-Dodecyl-4(1H)Quinolone, a High-Affinity Inhibitor of Alternative (Type II) NADH Dehydrogenases. *Antimicrobial Agents and Chemotherapy* **51**:1217-22

Schindelin Johannes, Arganda-Carreras Ignacio, Frise Erwin, Kaynig Verena, Longair Mark, Pietzsch Tobias, Preibisch Stephan, et al. (2012) Fiji: An Open-Source Platform for Biological-Image Analysis. *Nature Methods* **9**:676-82

Shaker Bilal, Yu Myeong-Sang, Song Jin Sook, Ahn Sunjoo, Ryu Jae Yong, Oh Kwang-Seok, Na Dokyun (2020) LightBBB: Computational Prediction Model of Blood–Brain-Barrier Penetration Based on LightGBM. *Bioinformatics* **37**:1135-39

Sharifiyazdi Hassan, Namazi Fatemah, Oryan Ahmad, Shahriari Reza, Razavi Mostafa (2012) Point Mutations in the Theileria Annulata Cytochrome b Gene Is Associated with Buparvaquone Treatment Failure. *Veterinary Parasitology* **187**:431-35

Shiomi K., Kiyono T., Okamura K., Uezumi M., Goto Y., Yasumoto S., Shimizu S., Hashimoto N. (2011) CDK4 and Cyclin D1 Allow Human Myogenic Cells to Recapture Growth Property without Compromising Differentiation Potential. *Gene Therapy* **18**:857-66

Shubar Hend M., Lachenmaier Sabrina, Heimesaat Markus M., Lohman Uwe, Mauludin Rachmat, Mueller Rainer H., Fitzner Rudolf, Borner Klaus, Liesenfeld Oliver (2011) SDS-Coated Atovaquone Nanosuspensions Show Improved Therapeutic Efficacy against Experimental Acquired and Reactivated Toxoplasmosis by Improving Passage of Gastrointestinal and Blood-Brain Barriers. *Journal of Drug Targeting* **19**:114-24

Shukla Anurag, Olszewski Kellen L., Llinás Manuel, Rommereim Leah M., Fox Barbara A., Bzik David J., Xia Dong, et al. (2018) Glycolysis Is Important for Optimal Asexual Growth and Formation of Mature Tissue Cysts by Toxoplasma Gondii. *International Journal for Parasitology* **48**:955-68

Smith David, Kannan Geetha, Coppens Isabelle, Wang Fengrong, Nguyen Hoa Mai, Cerutti Aude, Olafsson Einar B., et al. (2021) Toxoplasma TgATG9 Is Critical for Autophagy and Long-Term Persistence in Tissue Cysts. *eLife* **10**:April https://doi.org/10.7554/eLife.59384

Song Zehua, Iorga Bogdan I., Mounkoro Pierre, Fisher Nicholas, Meunier Brigitte (2018) The Antimalarial Compound ELQ-400 Is an Unusual Inhibitor of the Bc1 Complex, Targeting Both Qo and Qi Sites. *FEBS Letters* **592**:1346-56

Songsungthong Warangkhana, Prasopporn Sunisa, Bohan Louise, Srimanote Potjanee, Leartsakulpanich Ubolsree, Yongkiettrakul Suganya (2021) A Novel Bicyclic 2,4-Diaminopyrimidine Inhibitor of Streptococcus Suis Dihydrofolate Reductase. *PeerJ* **9**:e10743

Songsungthong Warangkhana, Yongkiettrakul Suganya, Bohan Louise E., Nicholson Eric S., Prasopporn Sunisa, Chaiyen Pimchai, Leartsakulpanich Ubolsree (2019) Diaminoquinazoline MMV675968 from Pathogen Box Inhibits Acinetobacter Baumannii Growth through Targeting of Dihydrofolate Reductase. *Scientific Reports* **9**:15625

Spalenka Jérémy, Escotte-Binet Sandie, Bakiri Ali, Hubert Jane, Renault Jean-Hugues, Velard Frédéric, Duchateau Simon, Aubert Dominique, Huguenin Antoine, Villena Isabelle (2018) Discovery of New Inhibitors of Toxoplasma Gondii via the Pathogen Box. *Antimicrobial Agents and Chemotherapy* **62** https://doi.org/10.1128/AAC.01640-17

Sun Lijun, Wu Jiaxi, Du Fenghe, Chen Xiang, Chen Zhijian J. (2013) Cyclic GMP-AMP Synthase Is a Cytosolic DNA Sensor That Activates the Type I Interferon Pathway. *Science* **339**:786-91

Thomsen-Zieger Nadine, Schachtner Joachim, Seeber Frank (2003) Apicomplexan Parasites Contain a Single Lipoic Acid Synthase Located in the Plastid. *FEBS Letters* **547**:80-86

Vallières Cindy, Fisher Nicholas, Antoine Thomas, Al-Helal Mohammed, Stocks Paul, Berry Neil G., Lawrenson Alexandre S., et al. (2012) HDQ, a Potent Inhibitor of Plasmodium Falciparum Proliferation, Binds to the Quinone Reduction Site of the Cytochrome Bc1 Complex. *Antimicrobial Agents and Chemotherapy* **56**:3739-47

Veale Clinton G. L (2019) Unpacking the Pathogen Box-an Open Source Tool for Fighting Neglected Tropical Disease. *ChemMedChem* **14**:386-453

Vercesi A. E., Rodrigues C. O., Uyemura S. A., Zhong L., Moreno S. N. (1998) Respiration and Oxidative Phosphorylation in the Apicomplexan Parasite Toxoplasma Gondii. *The Journal of Biological Chemistry* **273**:31040-47

Vila Taissa, Lopez-Ribot Jose L. (2017) Screening the Pathogen Box for Identification of Candida Albicans Biofilm Inhibitors. *Antimicrobial Agents and Chemotherapy* **61** https://doi.org/10.1128/AAC.02006-16

Wang Jin-Lei, Huang Si-Yang, Behnke Michael S., Chen Kai, Shen Bang, Zhu Xing-Quan (2016) The Past, Present, and Future of Genetic Manipulation in Toxoplasma Gondii. *Trends in Parasitology* **32**:542-53

Wang Peiyan, Li Siji, Zhao Yingchi, Zhang Baohuan, Li Yunfei, Liu Shengde, Du Hongqiang, et al. (2019) The GRA15 Protein from Toxoplasma Gondii Enhances Host Defense Responses by Activating the Interferon Stimulator STING. *The Journal of Biological Chemistry* **294**:16494-508

Weiss Louis M., Dubey Jitender P. (2009) Toxoplasmosis: A History of Clinical Observations. *International Journal for Parasitology* **39**:895-901

Winder W. W., Hardie D. G. (1999) AMP-Activated Protein Kinase, a Metabolic Master Switch: Possible Roles in Type 2 Diabetes. *The American Journal of Physiology* **277**:E1-10

Winzer Pablo, Müller Joachim, Aguado-Martínez Adriana, Rahman Mahbubur, Balmer Vreni, Manser Vera, Ortega-Mora Luis Miguel, et al. (2015) In Vitro and In Vivo Effects of the Bumped Kinase Inhibitor 1294 in the Related Cyst-Forming Apicomplexans Toxoplasma Gondii and Neospora Caninum. *Antimicrobial Agents and Chemotherapy* **59**:6361-74

Zampieri Mattia, Zimmermann Michael, Claassen Manfred, Sauer Uwe (2017) Nontargeted Metabolomics Reveals the Multilevel Response to Antibiotic Perturbations. *Cell Reports* **19**:1214-28

Deborah Maus, Martin Blume (2025) Screening the MMV Pathogen Box reveals the mitochondrial bc1-complex as a drug target in mature Toxoplasma gondii bradyzoites. massIVE. ID MSV000100157 ftp://massive-ftp.ucsd.edu/v11/MSV000100157/

Peer reviews

Reviewer #1 (Public review):

Summary:

The authors' goal was to advance the understanding of metabolic flux in the bradyzoite cyst form of the parasite T. gondii, since this is a major form of transmission of this ubiquitous parasite, but very little is understood about cyst metabolism and growth.

Nonetheless, this is an important advance in understanding and targeting bradyzoite growth.

Strengths:

The study used a newly developed technique for growing T. gondii cystic parasites in a human muscle-cell myotube format, which enables culturing and analysis of cysts. This enabled screening of a set of anti-parasitic compounds to identify those that inhibit growth in both vegetative (tachyzoite) forms and bradyzoites (cysts). Three of these compounds were used for comparative Metabolomic profiling to demonstrate differences in metabolism between the two cellular forms.

One of the compounds yielded a pattern consistent with targeting the mitochondrial bc1 complex, and suggest a role for this complex in metabolism in the bradyzoite form, an important advance in understanding this life stage.

Weaknesses:

Studies such as these provide important insights into the overall metabolic differences between different life stages, and they also underscore the challenge with interpreting individual patterns caused by metabolic inhibitors due to the systemic level of some of some targets, so that some observed effects are indirect consequences of the inhibitor action. While the authors make a compelling argument for focusing on the role of the bc1 complex, there are some inconsistencies in the some patterns that underscore the complexity of metabolic systems.

https://doi.org/10.7554/eLife.102511.2.sa3

Reviewer #2 (Public review):

Summary:

A particular challenge in treating infections caused by the parasite Toxoplasma gondii is to target (and ultimately clear) the tissue cysts that persist for the lifetime of an infected individual. The study by Maus and colleagues leverages the development of a powerful in vitro culture system for the cyst-forming bradyzoite stage of Toxoplasma parasites to screen a compound library for candidate inhibitors of parasite proliferation and survival. They identify numerous inhibitors capable of inhibiting both the disease-causing tachyzoite and the cyst-forming bradyzoite stages of the parasite. To characterize the potential targets of some of these inhibitors, they undertake metabolomic analyses. The metabolic signatures from these analyses lead them to identify one compound (MMV1028806) that interferes with aspects of parasite mitochondrial metabolism. In the revised version of the manuscript, the authors present convincing evidence that MMV1028806 targets the mitochondrial electron transport (ETC) chain of the parasite (although they don't identify the actual target in the ETC). The revised manuscript also nicely addresses my other criticisms of the original version. Overall, the study presents an exciting approach for identifying and characterizing much-needed inhibitors for targeting tissue cysts in these parasites.

Strengths:

The study presents convincing proof-of-principle evidence that the myotube-based in vitro culture system for T. gondii bradyzoites can be used to screen compound libraries, enabling the identification of compounds that target the proliferation and/or survival of this stage of the parasite. The study also utilizes metabolomic approaches to characterize metabolic 'signatures' that provide clues to the potential targets of candidate inhibitors. In addition to insights into candidate bradyzoite inhibitors, the study also provides new insights into the physiological role of the mitochondrial electron transport chain of bradyzoites, and raises a host of interesting questions around the functional roles of mitochondria in this stage of the parasite.

Weaknesses:

In the revised manuscript, the authors have included additional oxygen consumption rate data that indicate that MMV1028806 targets the mitochondrial electron transport chain (ETC). These data are convincing. On line 481, the authors state that "treatments with ATQ, BPQ, MMV1028806, and antimycin A resulted in substantially reduced oxygen consumption levels relative to the DMSO control and suggest indeed a blockage of the mETC consistent with the inhibition of the bc1-complex." The OCR assay the authors use is still only an indirect measure of bc1 activity. Given that most OCR-inhibiting compounds in T. gondii are bc1 inhibitors, it is possible (and perhaps likely) that MMV1028806 is targeting this complex. However, the data cannot rule out that it is targeting another component of the ETC (or potentially even a TCA cycle enzyme). Without a direct test that MMV1028806 inhibits bc1 complex activity, the authors should be more cautious in their interpretation (e.g. by

acknowledging the limitations of their conclusion, or acknowledging other possible targets). Similarly, the conclusion on line Line 622 that "... we confirmed the bc1-complex as a target" is overstating the findings. The phrasing on lines 683-695 is more appropriate: "... suggesting that it also targets complex III or a functionally linked site within the mitochondrial electron transport chain."

https://doi.org/10.7554/eLife.102511.2.sa2

Reviewer #3 (Public review):

Summary:

The authors described an exciting 400-drug screening using a MMV pathogen box to select compounds that effectively affect the medically important Toxoplasma parasite bradyzoite stage. This work utilises a bradyzoites culture technique that was published recently by the same group. They focused on compounds that affected directly the mitochondria electron transport chain (mETC) bc1-complex and compared with other bc1 inhibitors described in the literature such as atovaquone and HDQs. They further provide metabolomics analysis of inhibited parasites which serves to provide support for the target and to characterise the outcome of the different inhibitors.

Strengths:

This work is important as, until now, there are no effective drugs that clear cysts during T. gondii infection. So, the discovery of new inhibitors that are effective against this parasite-stage in culture and thus have the potential to battle chronic infection is needed. The further metabolic characterization provides indirect target validation and highlight different metabolic outcome for different inhibitors. The latter forms the basis for new studies in the field to understand the mode of inhibition and mechanism of bc1-complex function in detail.

The authors focused in the function of one compound, MMV1028806, that is demonstrated to have a similar metabolic outcome to burvaquone. Furthermore, the authors evaluated the importance of ATP production in tachyzoite and bradyzoites stages and under atovaquone/HDQs drugs.

https://doi.org/10.7554/eLife.102511.2.sa1

Author response:

The following is the authors' response to the original reviews.

> ***Public Reviews:***
>
> ***Reviewer #1 (Public review):***
>
> *Summary:*
>
> *The authors' goal was to advance the understanding of metabolic flux in the bradyzoite cyst form of the parasite T. gondii, since this is a major form of transmission of this ubiquitous parasite, but very little is understood about cyst metabolism and growth. Nonetheless, this is an important advance in understanding and targeting bradyzoite growth.*
>
> *Strengths:*
>
> *The study used a newly developed technique for growing T. gondii cystic parasites in a human muscle-cell myotube format, which enables culturing and analysis of cysts. This*

> *enabled the screening of a set of anti-parasitic compounds to identify those that inhibit growth in both vegetative (tachyzoite) forms and bradyzoites (cysts). Three of these compounds were used for comparative Metabolomic profiling to demonstrate differences in metabolism between the two cellular forms.*
>
> *One of the compounds yielded a pattern consistent with targeting the mitochondrial bc1 complex and suggests a role for this complex in metabolism in the bradyzoite form, an important advance in understanding this life stage.*
>
> *Weaknesses:*
>
> *Studies such as these provide important insights into the overall metabolic differences between different life stages, and they also underscore the challenge of interpreting individual patterns caused by metabolic inhibitors due to the systemic level of some of the targets, so that some observed effects are indirect consequences of the inhibitor action. While the authors make a compelling argument for focusing on the role of the bc1 complex, there are some inconsistencies in the patterns that underscore the complexity of metabolic systems.*

We agree with reviewer #1 that metabolic fingerprints are complex to interpret and we did try to approach this problem by including mock treatment and non-metabolic inhibitors as controls. We address specific concerns below.

> ***Reviewer #2 (Public review):***
>
> *Summary:*
>
> *A particular challenge in treating infections caused by the parasite Toxoplasma gondii is to target (and ultimately clear) the tissue cysts that persist for the lifetime of an infected individual. The study by Maus and colleagues leverages the development of a powerful in vitro culture system for the cyst-forming bradyzoite stage of Toxoplasma parasites to screen a compound library for candidate inhibitors of parasite proliferation and survival. They identify numerous inhibitors capable of inhibiting both the disease-causing tachyzoite and the cyst-forming bradyzoite stages of the parasite. To characterize the potential targets of some of these inhibitors, they undertake metabolomic analyses. The metabolic signatures from these analyses lead them to identify one compound (MMV1028806) that interferes with aspects of parasite mitochondrial metabolism. The authors claim that MV1028806 targets the bc1 complex of the mitochondrial electron transport chain of the parasite, although the evidence for this is indirect and speculative. Nevertheless, the study presents an exciting approach for identifying and characterizing much-needed inhibitors for targeting tissue cysts in these parasites.*
>
> *Strengths:*
>
> *The study presents convincing proof-of-principle evidence that the myotube-based in vitro culture system for T. gondii bradyzoites can be used to screen compound libraries, enabling the identification of compounds that target the proliferation and/or survival of this stage of the parasite. The study also utilizes metabolomic approaches to characterize metabolic 'signatures' that provide clues to the potential targets of candidate inhibitors, although falls short of identifying the actual targets.*
>
> *Weaknesses:*
>
> *(1) The authors claim to have identified a compound in their screen (MMV1028806) that targets the bc1 complex of the mitochondrial electron transport chain (ETC). The evidence they present for this claim is indirect (metabolomic signatures and changes in mitochondrial membrane potential) and could be explained by the compound targeting*

> *other components of the ETC or affecting mitochondrial biology or metabolism in other ways. In order to make the conclusion that MMV1028806 targets the bc1 complex, the authors should test specifically whether MMV1028806 inhibits bc1-complex activity (i.e. in a direct enzymatic assay for bc1 complex activity). Testing the activity of MMV1028806 against other mitochondrial dehydrogenases (e.g. dihydroorotate dehydrogenase) that feed electrons into the ETC might also provide valuable insights. The experiments the authors perform also do not directly measure whether MMV1028806 impairs ETC activity, and the authors could also test whether this compound inhibits mitochondrial O2 consumption (as would be expected for a bc1 inhibitor).*

We thank the reviewer for highlighting this important aspect. To further investigate the effect of MMV1028806 on the mETC, we adapted a commercial oxygen consumption assay and demonstrated that MMV1028806, like Atovaquone and Buparvaquone, inhibits the ETC, leading to reduced oxygen consumption similar to Antimycin A, which inhibits the bc1-complex. These results are now included in the revised manuscript (Methods, lines 210–233; Results, lines 460–468).

> *(2) The authors claim that compounds targeting bradyzoites have greater lipophilicity than other compounds in the library (and imply that these compounds also have greater gastrointestinal absorbability and permeability across the blood-brain barrier). While it is an attractive idea that lipophilicity influences drug targeting against bradyzoites, the effect seems pretty small and is complicated by the fact that the comparison is being made to compounds that are not active against parasites. If the authors are correct in their assertion that lipophilicity is a major determinant of bradyzoicidal compounds compared to compounds that target tachyzoites alone, you would expect that compounds that target tachyzoites alone would have lower lipophilicity than those that target bradyzoites. It would therefore make more sense to (statistically) compare the bradyzoicidal and dual-acting compounds to those that are only active in tachyzoites (visually the differences seem small in Figure S2B). This hypothesis would be better tested through a structure-activity relationship study of select compounds (which is beyond the scope of the study). Overall, the evidence the authors present that high lipophilicity is a determinant of bradyzoite targeting is not very convincing, and the authors should present their conclusions in a more cautious manner.*

Thank you for raising this excellent point. We performed a statistical test of tachyzoidal and both bradyzoidal and dually active compounds and find indeed no significant difference (P = 0.06). We altered the results text line 367-368 and the figure S2B caption to explicitly mention this.

> *(3) Page 11 and Figure 7. The authors claim that their data indicate that ATP is produced by the mitochondria of bradyzoites "independently of exogenous glucose and HDQ-target enzymes." The authors cite their previous study (Christiansen et al, 2022) as evidence that HDQ can enter bradyzoites, since HDQ causes a decrease in mitochondrial membrane potential. Membrane potential is linked to the synthesis of ATP via oxidative phosphorylation. If HDQ is really causing a depletion of membrane potential, is it surprising that the authors observe no decrease in ATP levels in these parasites? Testing the importance of HDQ-target enzymes using genetic approaches (e.g. gene knockout approaches) would provide better insights than the ATP measurements presented in the manuscript, although would require considerable extra work that may be beyond the scope of the study. Given that the authors' assay can't distinguish between ATP synthesized in the mitochondrion vs glycolysis, they may wish to interpret their data with greater caution.*

We thank the reviewer for addressing this important point. The enzymatic assay used in our study cannot distinguish whether ATP is produced via glycolysis or mitochondrial respiration. However, we minimized glycolytic ATP production in bradyzoites by starving

them for one week without glucose. After this period, amylopectin stores are depleted, forcing the parasites to utilize glutamine via the GABA shunt to fuel the TCA cycle and generate ATP predominantly through respiration. While minor ATP production via gluconeogenic fluxes cannot be excluded, the main ATP supply under these conditions is expected to originate from the mitochondrial electron transport chain. Indeed, ATP levels are lower in HDQ-treated bradyzoites, which we attribute to the compound's impact on electron-supplying enzymes upstream of the bc1 complex, although this inhibition is not sufficient to fully abolish ATP production as observed with Atovaquone treatment.

> ***Reviewer #3 (Public review):***
>
> *Summary:*
>
> *The authors describe an exciting 400-drug screening using a MMV pathogen box to select compounds that effectively affect the medically important Toxoplasma parasite bradyzoite stage. This work utilises a bradyzoites culture technique that was published recently by the same group. They focused on compounds that affected directly the mitochondria electron transport chain (mETC) bc1-complex and compared them with other bc1 inhibitors described in the literature such as atovaquone and HDQs. They further provide metabolomics analysis of inhibited parasites which serves to provide support for the target and to characterise the outcome of the different inhibitors.*
>
> *Strengths:*
>
> *This work is important as, until now, there are no effective drugs that clear cysts during T. gondii infection. So, the discovery of new inhibitors that are effective against this parasite stage in culture and thus have the potential to battle chronic infection is needed. The further metabolic characterization provides indirect target validation and highlights different metabolic outcomes for different inhibitors. The latter forms the basis for new studies in the field to understand the mode of inhibition and mechanism of bc1-complex function in detail.*
>
> *The authors focused on the function of one compound, MMV1028806, that is demonstrated to have a similar metabolic outcome to burvaquone. Furthermore, the authors evaluated the importance of ATP production in tachyzoite and bradyzoites stages and under atovaquone/HDQs drugs.*
>
> *Weaknesses:*
>
> *Although the authors did experiments to identify the metabolomic profile of the compounds and suggested bc-1 complex as the main target of MMV1028806, they did not provide experimental validation for that.*

In our updated manuscript we performed additional experiments such as oxygen consumption assay to further qualify the bc1 complex as the target. We also toned down some of our statements to make sure that no false claims are made.

> ***Recommendations for the authors:***
>
> ***Reviewer #1 (Recommendations for the authors):***
>
> *Introduction: It would be helpful to briefly describe what the pathogen Box is, what compounds are in it, and the rationale for using a drug screen to better understand mitochondrial function in cysts.*

Thank you for this suggestion, we added an introduction of the MMV pathogen box and outlined our rationale for our experimental approach in lines 90 to 99.

> *Please explain why dual-active drugs were useful for understanding differences, rather than just seeking drugs that might target bradyzoites alone.*

We focused on dually active compounds for two reasons. First, these are the most promising and potent targets to develop drugs against. Both stages might occur simultaneously and these dually active drugs may eliminate the need for treatment with a drug combination. Second, we speculated that monitoring the responses to inhibition of the same process in both parasite stages would reveal its functional consequences. Dually active compounds enable this direct comparison. Bradyzoite-specific compounds may be interesting from a developmental perspective but may require a reverse genetic follow-up to compare differences between stages. The lack of a well-established inducible expression system in bradyzoites that allows short term and synchronized knock-down makes metabolomic approaches difficult. We added these two points in brief to the results section (line 378 – 381).

> *Figure 4: this is a very important figure in understanding the significance of the work, but it is not well described in the legend. Even if these graphics have been used in other manuscripts, it would be helpful to provide better annotation in the figure legend.*

Thank you for pointing this out. We expanded the figure legend to explain the isotopologues data in more detail. Line 793 to 802.

> *B,D: Explain what the three columns for each drug category represent.*

Addressed

> *C,E: Explain what isotopologues are, what the M+ notation means, and what the pie charts represent. Other main figures have suitable legends.*

Addressed

> *Discussion: there are several places where the reasoning is a bit hard to follow, and rearrangement to provide a clear logical flow would be helpful. In particular, the reasoning for why HDQ impairs active but non-essential processes could be laid out more clearly.*

We added additional clarifications to the discussion section and re-wrote the HDQ paragraph. We hope that our reasoning is now easier to follow.

> *Abbreviations: A list of abbreviations for the entire manuscript would be helpful.*

This is a good idea and we now provide an abbreviations list.

> *Minor typos:*
>
> *P12, 2d paragraph: sentence beginning with: Consistent with this hypothesis... "cysts" is used twice*

Corrected

> *P15, top of the second paragraph: "nano" and "molar" should be one word*

Corrected

> ***Reviewer #2 (Recommendations for the authors):***
>
> *Major comments (not already covered in the weaknesses section of the public review)*
>
> *(1) Figure 2 and the related description of these experiments in the methods section (page 3). The approach for calculating IC50 values for the compounds against*

> *tachyzoites is unclear. How did the authors determine the time point for calculating IC50 vacuoles? Was this when the DMSO control wells reached maximum fluorescence? This could be described in a clearer manner. A concern with calculating IC50 values on different days is that parasites will have undergone more lytic cycles after 7 days compared to 4 days, which means that the IC50 values for fast- vs slow-acting compounds might be quite different between these days. As a more minor comment on these experiments, the methods section does not describe whether the test compound was removed after 7 days, as the experimental scheme in Figure S1A seems to imply. Please clarify in the methods section.*

This is a very good point and we clarified this in the methods section, line 157–160. In brief, we choose the latest time point when exponential growth could be observed in the fastest growing cultures, generally this was in mock treated cultures and at day 4 post infection. We also clarified that we changed media and removed treatment after 7 days.

> *Minor Comments*
>
> *(2) Page 2. "we employed a recently developed human myotube-based culture system to generate mature T. gondii drug-tolerant bradyzoites". What makes these bradyzoites 'drug-tolerant' or to which drugs are they tolerant? This isn't clear from the description.*

We added these details in the introduction (line 94 to 96) and state that these cysts develop resistance against anti-folates, bumped kinase inhibitors and HDQ, a Co-enzyme Q analog.

> *(3) Figure 1E. The number of compounds in this pie chart adds up to 384, whereas the methods describe that 371 compounds were tested. What explains this discrepancy in numbers?*

We understand the confusion. We now updated the pie chart to reflect only compounds that were included in the primary screen (371) as reflected in Supplementary Table S1. We separately analysed 29 compounds that were previously tested against tachyzoites by Spalenka et al., and found an additional 13 compound, that were originally included in the pie chart. In a secondary test the activity of 10 of these 13 compounds could be confirmed. All in all we found the 16 compounds shown in Fig. 2 E-G.

> *(4) Page 3. The resazurin assays for measuring host cell viability could be explained in a clearer manner. What host cells were used? Were the host cells confluent when the drug was added (and the assay conducted) or was the drug added when the host cells were first seeded? How long were the host cells cultured in the candidate inhibitors before the assays were performed? What concentration (or concentration range) were the compounds tested? The host inhibition data are not easily accessible to the reader - the authors might consider including these data as part of Table S2D.*

The necessary information was added to the methods section (line 145 to 153). We tested for host toxicity in both HFF and KD3 myotubes during the primary screen at 10 µM in triplicates. The colorimetric assay was performed after tachyzoite growth assays in HFFs 7 days post infection and after completion of the 4 week re-growth phase of bradyzoites in myotubes. The resulting data is already part of Supplementary File 1. In addition, we performed concentration dependent resazurin assays after secondary concentration dependent growth inhibition assays and also included data in Supplementary File 1. For the bradyzoite growth assay we performed visual inspection after drug exposure for one week and before tachyzoite re-growth to detect missing or damaged monolayer. Also, this data is included in the Supplementary File 1. We also included the cytotoxicity data as suggested into Table S2D.

> *(5) Page 7. "Except for four compounds (MMV021013, MMV022478, MMV658988, MMV659004), minimal lethal concentrations were higher in bradyzoites". The variation in*

> *these data seems quite large to be making this claim. Consider a statistical analysis of these data to compare potencies in tachyzoites vs bradyzoites.*

With this sentence we aimed to describe the results and not to make a statement. We toned down the sentence to "… minimal lethal concentrations appear generally higher in bradyzoites… " line 344 to 347. We also added a line 1 µM in the charts to facilitate easier comparison of compound efficacies.

> *(6) It would be helpful to readers to include the structures of hit compounds in the figures (perhaps as part of Figure 3).*

This is a good idea and would improve the manuscript. To not overburden figure 3 we added structures to Fig S3.

> *(7) Page 8. "Infected monolayers were treated for three hours with a 3-fold of respective IC50 concentrations". 3-fold higher than IC50 concentrations? This isn't clear.*

Thank you for noticing this: We clarified the sentence and also corrected the concentration, corresponding to five times their IC50s as stated in the methods section: "Infected monolayers were treated for three hours with compound concentrations five times their respective IC_{50} values or the solvent DMSO." Line 374 - 376

> *(8) Page 9. "buparvaquone, which we found to be dually active against T. gondii tachyzoites and bradyzoites, targets the bc1-complex in Theileria annulata (McHardy et al. 1985) and Neospora caninum (Müller et al. 2015) and was recently found active against T. gondii tachyzoites (Hayward et al. 2023)." The latter paper showed that buparvaquone targets the bc1 complex in T. gondii tachyzoites as well.*

Yes, it was found to inhibit O2 consumption rate in tachyzoites. We changed the sentence accordingly. Line 407 to 411.

> *(9) Page 9. "Anaplerotic substrates were also affected by all three treatments, most notably a strong accumulation of aspartic acid." It is interesting that the M+3 isotopologue of aspartate (presumably synthesised from pyruvate) is the predominant form (rather than the M+2 and M+4 isotopologues that would derive from the TCA cycle, and as the diagram in Figure 4A seems to suggest). Given that aspartate is a precursor of pyrimidine biosynthesis that is upstream of the DHODH reaction, it is conceivable that its accumulation is related to the depletion of pyrimidine biosynthesis (so would tie into the point about the accumulation of DHO and CarbAsp noted earlier in the paragraph).*

Yes, we assume the same. We altered the text and summarized the changes in Asp as a result of DHOD inhibition, as we also already do in the next paragraph using ^{15}N-glutamine labelling. Line: 416 - 418

> *(10) Figure 6 and Page 10. Regarding the metabolomic experiments that show increased levels of acyl-carnitines. The authors note that "Since [beta-oxidation] is thought to be absent in T. gondii, we attribute these changes to inhibition of host mitochondria". This is conceivable, although the T. gondii genome does encode homologs of the proteins necessary for beta-oxidation (e.g. see PMID 35298557). If the carnitine is coming from host mitochondria, is host contamination a concern for interpreting the metabolomic data? Or do the authors think that parasites are scavenging carnitine from host cells? It is curious that the carnitine accumulation is observed in parasites treated with buparvaquone (and MMV1028806) but not atovaquone, even though buparvaquone and atovaquone (and possibly MMV1028806) target the same enzyme. Do the authors have any thoughts on why that might be the case?*

Yes, thank you for raising this point. We changed the discussion elaborating on this and included the debated presence of beta-oxidation: line 640: “We also detect elevated levels of acyl-carnitines in BPQ and MMV1028806 treated bradyzoites. These molecules act as shuttles for the mitochondrial import of fatty acids for β-oxidation. However, this pathway has not been shown to be active and is deemed absent in *T. gondii* (35298557, 18775675). The presence of acyl-carnitines in bradyzoites might reflect import from the host. It is conceivable that their elevation in response to buparvaquone and MMV1028806 indicates compromised functionality of the host bc1-complex and subsequently accumulating β-oxidation substrates. Indeed, BPQ has a very broad activity across Apicomplexa (Hudson et al. 1985) and kinetoplastids (Croft et al. 1992).“ Regarding the existence of beta-oxidation: some potential enzymes might be conserved, but those could in part take part in branched chain amino acid degradation pathways. On a separate note: we looked extensively on beta-oxidation using stable isotope labelling and became convinced that any activity occurred in the host cell only but not in the parasite (unpublished).

> *(11) Page 11. "the mitochondrial [electron] transport chain in bradyzoites".*

Corrected.

> *(12) Figure S6B. Were these optimization experiments performed in tachyzoites or bradyzoites? If the former, and given that bradyzoites have apparently smaller amounts of ATP per parasite (Figure 7C), are these values in the linear range for 10^5 bradyzoites?*

Yes, we do think that the assay remains linear for these lower concentrations. Tachyzoites give a linear response starting from 10^3 parasites per sample. In the actual experiment we used 10^5 parasites, both tachyzoites and bradyzoites. Under the tested conditions bradyzoites maintain 10% of the ATP pools of tachyzoites, which should be well within the linear range of the assay. Also in Atovaquone-treated bradyzoites ATP concentration could be lower to 10% and still remain in the linear range of the assay. For practical reasons, we simply acknowledge this limitation and consider it acceptable within the scope of this study.

> ***Reviewer #3 (Recommendations for the authors):***
>
> *Major comments*
>
> *(1) The authors should provide a negative control for the experiment on Figure 5. I would suggest doing the same experiment with an inhibitor that has no effect on mitochondrial potential.*

We addressed this criticism by repeating the assay on tachyzoites and additionally including inhibitors that do not have the mitochondrial electron transport chain as their primary target (Pyrimethamine, Clindamycin, 6-Diazo-5-oxo-L-norleucin). The results are summarized in the supplementary Fig S5, line 445 – 449) and show that there is no effect of these inhibitors on the mitochondrial membrane potential. This supports the specificity of the assay and suggests that MMV1028806 and BPQ indeed target a mitochondrial process in this stage. Also, in this repetition ATQ, BPQ and MMV1028806 did significantly deplete the Mitotracker signal.

> *(2) Figure 5 - Did the authors perform this experiment in 3 biological replicates? This requires clarification of the figure legend.*

No, we did not perform the experiment in 3 biological replicates. After establishing the assay thoroughly, we performed it once on tachyzoites and bradyzoites. The sampling was done on every vacuole we encountered during microscopy going through the slide from left to right. That is the reason the sample size varies from treatment to treatment. The sample size is mentioned in the caption of figure 5. However, we repeated the experiment with additional

controls (see Fig. S5), which showed that the Mitotracker signals were significantly depleted in a very similar manner in ATQ, BPQ and MMV1028806 treated parasites.

> *(3) The authors identify that MMV1028806 has bc1-complex as the main target. I suggest that they should perform a complex III activity assay to affirm this. Also, it would be good to test if other mETC complexes are affected by this compound to prove its specificity. There is only one paper showing complex III activity in tachyzoites (PMID:37471441) and no papers in bradyzoites. So if the authors cannot do this assay, I suggest that they should change the text indicating that bc-1 complex could be the main target of the compound but more experimental validation is needed.*

We hope to have satisfied the reviewer's request by performing an oxygen consumption assay on tachyzoites. Together with metabolic profiling and labelling data, this shows that both upstream and downstream processes are impacted by MMV1028806 and strongly suggest the bc1-complex as a target (Fig 5E).

> *(4) Figure S5 - Are the differences shown in the EM experiment statistically supported?*

We analyzed 28 images and measured the areas in 12 to 26 images. We substituted the table of means in Fig S6B by a graph showing individual values. These areas are indeed statistically different between DMSO and ATQ / MMV treated parasites. We changed the wording in the results section accordingly "Analysis by thin section electron microscopy revealed a largely unaffected sub-mitochondrial ultrastructure but the areas of mitochondrial profiles were changed in comparison to control after exposure with ATQ and MMV1028806 but not with BPQ (Fig. S6)". The description of Fig S6B was changed to "(B) Measured areas of mitochondrial profiles from 21, 12, 15 and 26 images showing DMSO, ATQ, BPQ and MMV1028806 treated parasites (* denotes $p < 0.05$ in Mann-Whitney tests)".

> *Minor comments:*
>
> *(1) What was the criteria to choose the example compounds in Figure 1B and 1D? The authors should clarify this in the text.*

These graphs are shown for illustrative purposes and were chosen based on their display of different drug efficacies. We considered this helpful for interpreting the screening data.

> *(2) Figure 2G - add statistical analysis.*

We added Mann-Whitney tests and updated the figure legend and results text accordingly in line 344 – 347.

> *(3) The authors should provide more insights in the discussion about why this new compound is the next step in drug discovery compared to atovaquone or burvaquone - for example, do you expect better availability in the brain, etc.*

We used MMV1028806 and the other hits ATQ and BPQ to make the point that the bc1-complex is a good target in bradyzoites that allows curative treatment. We do not suggest that the compound itself is a good starting point. We point to other actively developed candidates such as ELQ series in the discussion, line 719.

> *(4) Scale bars in Figure 5 should be aligned and have equal thickness.*

We re-formatted the scale bars and aligned them when not obscuring parasites.

> *(5) The authors should be consistent with font sizes and styles in all the figures.*

We adjusted the font styles to match each other.

https://doi.org/10.7554/eLife.102511.2.sa0